THE ABSORPTION OF COSMIC RAYS

AND

THE PRODUCTION OF KNOCK-ON SECONDARIES

THE ABSORPTION OF COSMIC RAYS
AND
THE PRODUCTION OF KNOCK-ON SECONDARIES

By

GERALD LESTER KEECH, M.Sc.

A Thesis

Submitted to the Faculty of Arts and Science

for the Degree

Doctor of Philosophy

McMaster University

October 1956

DOCTOR OF PHILOSOPHY (1956) McMASTER UNIVERSITY
(Physics) Hamilton, Ontario

TITLE: The Absorption of Cosmic Rays and the Production of Knock-on Secondaries

AUTHOR: Gerald Lester Keech, B.A.Sc. (University of Toronto)
M.Sc. (McMaster University)

SUPERVISOR: The late Professor Fricis Gulbis

NUMBER OF PAGES: 120

SCOPE AND CONTENTS:

This thesis describes two investigations of cosmic-ray phenomena. The first was designed to check the existence of a previously observed anomaly in the absorption of cosmic rays in lead (58). The results indicate that within 1% there is no such anomaly and suggest reasons for its appearance in the earlier work.

The second represents an investigation of the frequency with which knock-on secondaries are produced by penetrating particles passing through aluminum as a function of the aluminum thickness. By indirect arguments it is inferred that the physical events represent the production of knock-on electrons by mu-mesons. Therefore, the expected form of thickness variation in the knock-on process is calculated using the orbital-electron - mu-meson collision probability (86, 87) and the sea-level mu-meson momentum spectrum (88, 89). The results establish an agreement between the experimental and calculated frequency to within 5% for aluminum thicknesses from 0 to 12 gm.-cm.$^{-2}$.

ACKNOWLEDGEMENT

I wish to acknowledge my profound debt to my Research Director, the late Professor F. Gulbis, not only for his advice and guidance which were indispensable in carrying out this work, but also for arousing and stimulating my curiosity concerning the fundamentals of physics and natural philosophy.

The completion of this work has been made possible by the continuing interest and constructive criticism of the members of my Supervisory Committee, Dr. A. B. McLay and Dr. H. G. Thode, to whom I express my sincerest gratitude.

Also, I am indebted to Dr. H. E. Johns for many valuable discussions and helpful suggestions, and to Mr. E. P. Hincks of Atomic Energy of Canada for drawing to my attention the possible effects of air showers upon the results.

Special thanks are extended to the Shell Oil Company and to the National Research Council for financial aid, in the form of research fellowships, during the period of the investigation.

TABLE OF CONTENTS

TABLE OF CONTENTS, Cont'd.

LIST OF FIGURES

LIST OF TABLES

CHAPTER I

GENERAL INTRODUCTION

At the beginning of this century, it was discovered that an electroscope, no matter how carefully insulated, shielded, and freed from radio-active contamination, gradually lost its charge (1). This finding led to the tentative suggestion that the ionizing agency responsible might be an extremely penetrating radiation of extra-terrestrial origin. In the years that followed many experiments were carried out to determine whether the source of radiation was terrestrial or not. It required over twenty years of experimentation by many workers to accumulate sufficient data to make universal the acceptance of the fact that the radiation originated outside the earth. Excellent accounts of the gradual amassing of experimental facts that led to an understanding of this cosmic radiation can be found in the standard texts dealing with this subject such as those listed in the Bibliography. Therefore only a brief account will be given here.

The earliest conclusive demonstration that the radiation is extraterrestrial is that of V. F. Hess in 1912 (2) and his results were confirmed shortly afterwards by W. Kolhorster (3). By means of balloons, they took ionization chambers to great heights and showed that the ionization increased with height above the earth's

surface. Another important confirmation that the radiation was not natural radioactivity in the earth's crust was obtained by Millikan and Cameron (4) when, in 1928, they lowered sealed electroscopes to various depths below the surface of snow-fed mountain lakes, which would be relatively free of natural radioactive substances. They found that the ionization fell off rapidly in the first meter or so and thereafter decreased more slowly with increasing depth.

A new era of investigation was initiated around 1928 with the development of the Geiger counter (5). This was especially useful when counters in a geometrical arrangement were operated in coincidence. By this means a beam of incoming particles is defined and hence the instrument is referred to as a cosmic ray telescope. The development of counter and counting circuits has progressed at such a rapid rate that the literature is now full of references to circuits and their application for coincidence, anticoincidence, and delayed coincidence arrangements.

A second instrument which made the new era so fruitful was the Wilson cloud chamber (6). This instrument became particularly versatile after the development of a counter control for the expansion of the chamber (7) thereby insuring, and even allowing a certain selection of cosmic ray events.

With the aid of the new instruments, it was soon established (8, 9) that charged particles were present among the cosmic rays observed within the earth's atmosphere. The following year Skobelzyn (10) observed evidence of showers of particles, that is, several associated rays passing simultaneously through the chamber. However, it was not yet clear that these particles were anything other than electrons secondary to gamma rays. This belief was particularly attractive after the discovery of the positive electron by C. D. Anderson in 1932 (11). It was immediately realized that the positron could be interpreted on the basis of Dirac's theoretically predicted negative energy states of the electron. The concept of the production of electron pairs by photons and of radiative collisions of electrons was a powerful stimulus to both theory and experiment. This was particularly so in the study of shower phenomena. The shower-production curve, that is, the number of showers detected as a function of the thickness of absorber above the apparatus was investigated by B. Rossi (12) (the curve has come to be known as the Rossi curve). He found that the number of showers increased initially with thickness of absorber, passing through a maximum before falling to a constant value. The experimental work was followed by a quantitative explanation in 1937 by H. J. Bhabha and W. Heitler (13) according to which showers consist of positive and negative electrons,

together with photons, and are developed by an alternating succession of radiative collisions and pair productions. This picture of shower production has come to be generally accepted, and is one of the most important concepts in the analysis of cosmic ray effects.

The assumption that the only charged particles in the cosmic radiation were positive and negative electrons gave rise to a dilemma in the interpretation of the absorption measurements of the radiation. It was found that the absorption in lead was greater for the first 10 cm. than for larger thickness; then at this thickness there was a rather sudden increase in the penetrating power of the radiation. This led to an empirical separation of the charged particles into a "soft component" (unable to penetrate 10 cm. of Pb) and a "hard component" (capable of traversing 10 cm. of Pb) (14). This distinction between hard and soft components would seem somewhat artificial if it were not that the two components also act differently in other ways. From observations by a number of investigators the following distinguishable characteristics were noted.

(i) The soft component produces showers in a few centimeters of lead while the hard component produces showers much less frequently in this range of thicknesses.

(ii) The intensity of the soft component rapidly

increases with altitude and drops rapidly underground, while the hard component exhibits a much slower variation with altitude and depth underground.

(iii) The absorption per atom of the soft component is proportional to Z^2, that is behaves in accordance with the quantum theory of radiation, while the absorption per atom of the hard component is proportional to Z, that is, it loses energy at a rate which can be accounted for by ionization only.

It seemed clear that the shower particles consist of electrons, while the penetrating particles have some property different from electrons. Furthermore the hard particles could not be protons since they ionize more lightly than protons of the same momentum. Thus the working hypothesis was put forth that there exist positive and negative singly-charged particles of mass intermediate between those of protons and electrons (15). Further determinations of mass by range-momentum and other direct means have led to general acceptance of the existence of the intermediate particle which now bears the name meson.

Such a belief, would not, perhaps, have been accepted so readily except for the fact that certain theoretical arguments had already been advanced by H. Yukawa (16) to explain intranuclear forces, which had

caused the existence of such a particle to be suspected.

To explain beta-decay in the Yukawa scheme it was necessary to postulate a radioactive decay of the theoretical particle into an electron and a neutrino. If one is to identify the particle postulated by Yukawa with the particle observed in cosmic rays, the latter as well must decay radioactively. The fact that it is unstable was inferred indirectly from the observed anomalously large absorption of mesons in a large column of the atmosphere compared with that in a short column of dense absorber of the same stopping power (17). Later the disintegration was shown directly in cloud chamber photographs by E. J. Williams and C. E. Roberts (18). The first successful direct measurement of the meson lifetime by the method of delayed coincidences was made in 1941 by F. Rasetti (19), who obtained a value near two microseconds, the presently accepted figure.

For a time it was widely accepted that the Yukawa particle and the cosmic-ray particle were the same, but with some reservation since the experimental lifetime was much longer than predicted by the theory. Then an indisputable refutation of the identification of the cosmic-ray meson with the Yukawa particle was given by the well-known experiment of Conversi, Pancini, and Piccioni (20), which showed that while in a heavy element (iron) only positive mesons decay, in a light element (carbon)

on the other hand, both positive and negative mesons decay. This result and subsequent confirmatory experiments by other workers, lead to the conclusion that the interaction between the meson and the nucleus is several orders of magnitude less than that required for the Yukawa particle, and so precludes the possibility of their identity.

Fortunately, in the same year C. F. Powell and co-workers reported finding tracks of a new particle whose mass was somewhat greater than that accepted for the meson (21). Their experimental technique consists of the development and analysis of tracks caused by the mesons in photographic emulsions. The use of special "nuclear" emulsions (22) has proven to be a most fruitful method of studying cosmic radiation, especially for the study of phenomena of low frequency of occurence, since the plates are continuously sensitive throughout any desired period of exposure.

Concurrent with the discovery of these new particles was the observation that they sometimes lead to the production of secondary mesons. This was found to be a common mode of decay and suggested that it is a fundamental process. The secondary meson was identified with the previously known meson and is given the name mu-meson while the heavier primary meson is denoted as a pi-meson. It was also found that the pi-meson has a strong interaction

with nucleons. This fact coupled with the much shorter mean lifetime of the pi-meson (23) has made it very attractive to identify the pi-mesons with the field particles in Yukawa's theory of nuclear forces.

Since the mesons are unstable, it is obvious that they must be produced in the earth's atmosphere by some primary radiation. The first insight as to the nature of this primary radiation was given by the discovery of the geomagnetic effects. The earliest discovered of these was the latitude effect, i.e., it was found that the cosmic ray intensity varied with change in geomagnetic latitude (24). Near sea level the latitude effect amounts to about a ten per cent decrease from high latitudes to the geomagnetic equator. The great significance of this latitude effect is that it demonstrates that at least some primaries are charged and that they come from outside the earth's atmosphere.

It is only with these assumptions that the observed latitude effect can be accounted for naturally. The explanation is that the magnetic field of the earth deflects the low energy particles in the primary radiation away from the earth near the geomagnetic equator, but the particles are able to reach the earth near the geomagnetic poles. That the particles must come from outside the earth's atmosphere is obvious because the magnetic deflection within the relatively small extension

of the earth's atmosphere will be slight.

The second geomagnetic effect that is of importance in revealing the nature of the primaries is the east-west effect, i.e., the difference between the number of particles coming from the eastern and from the western directions. This effect is due to the fact that a positive particle with low momentum will be able to reach the earth more easily from the west than from the east, whereas these directions will be interchanged for a negative particle. Successful measurement of the east-west effect by T. H. Johnson and collaborators (25) led to the deduction that most, if not all, of the primary radiation is positive. With these findings the natural hypothesis is that the primary radiation consists chiefly of protons, which interact with air atoms in the upper atmosphere to form the penetrating mesons.

In 1941 Schien, et al. (26) showed that most of the particles near the upper most region of the atmosphere have, in fact, the characteristics of protons. This afforded experimental confirmation of the general belief that the primary cosmic radiation consists almost exclusively of protons. Then in 1948 Freir, et al. (27) observed the tracks of very heavy nuclei of large penetrating power in nuclear emulsions exposed in a stratospheric balloon flight. They showed that these nuclei could not have been produced by collision of primary

protons with air atoms. Thus it was concluded that heavy nuclei were part of the primary cosmic radiation. Since that time further work has revealed that stripped nuclei of atoms heavier than hydrogen contribute about 15 per cent of the total flux of primary particles. In all, they contribute about 30% of the incident protons and all the incidence neutrons, 40% of the incident energy, and 50% of the ionization in the upper atmosphere.

The origin of the primary radiation still remains mostly speculative. The difficulty in forming any hypothesis is to account for the very high individual energies of the particles and for the chemical composition of the radiation. Because of the temporary nature and incompleteness of the various theories concerning the origin they will not be discussed here.

Upon entering the earth's atmosphere, the primary radiation interacts very strongly with the nuclei of the air atoms. Because of the collisions with the atmospheric nuclei the primary radiation is soon absorbed. The heavy particles are broken up and give rise to fragments of smaller size and to free nucleons. The mean free path which characterizes these collisions depends on the kind of colliding nuclei and decreases as the atomic number increases. The collision length varies from 45 gm. cm.$^{-2}$ for atomic number 2 to 21 gm. cm.$^{-2}$ for atomic number 14 (28). Thus the heavy component is very rapidly absorbed

as compared with the proton component, the mean free path of which is 120 gm. cm.$^{-2}$. Therefore one would expect the maximum production of secondary radiation at a height of about 15 - 20 kilometers above sea level, since this corresponds to a thickness of 50 - 100 gm. cm.$^{-2}$ of atmosphere traversed by the primary radiation. Early experiments on mesons have established that the majority are produced at about this height (29) but with some production down to moderate altitudes (30).

The nuclear interactions manifest themselves as "stars" in nuclear emulsions and cloud chambers (31, 32) and are detected as penetrating showers by counter telescopes (33).

All of the known fundamental particles are freed or created in these nuclear explosions. Besides the well established light or L-mesons, protons and neutrons, there are heavy or K-mesons and hyperons. The K-mesons are particles with masses intermediate between that of the pi-meson and neutron, while hyperons have masses intermediate between that of the proton and deuteron. The K-mesons and hyperons are highly unstable, decaying into L-mesons and nucleons.

Since the pi-mesons and nucleons are by far in the majority and since the details concerning the K-mesons and hyperons are only just beginning to be unravelled, they will not be considered here; instead the reader is

referred to the paper by M. Deutschman (34).

The pi-mesons are both charged and uncharged. The charges of the mesons can be of either sign. They have a mass of 273 electron masses (35) and a mean lifetime of $2.5 \cdot 10^{-8}$ seconds (36)and decay into a mu-meson and a neutrino (37). The neutral pi-meson has a mass of 264 electron masses (38) and a mean lifetime $\sim 10^{-14}$ seconds giving rise to two photons (39, 40). The spin of both the charged (41, 42) and neutral pi-meson (43) are believed to be zero.

The generation of pi-mesons in nuclear collisions, both by the primary radiation and by secondary nucleons may be considered as the main event of the whole phenomenology of cosmic rays. The pi-mesons serve as a link between the primary component and the two secondary components. The mu-component originates from the decay of the charged pi-meson and the neutral pi-meson generates a fraction of the soft component by decaying into two photons which in turn create an electron-photon cascade. The pi-mesons themselves do not contribute notably to the secondary radiation since their very short life makes their direct contribution to observable effects very small. As has already been noted, the production of the pi-mesons occurs chiefly at a height of about 15 - 20 kilometers above sea level but there will be some production throughout the atmosphere. This is evidenced by the observations of

penetrating shower frequency with altitude (44). This production will be chiefly due to the secondary nucleonic component.

The mu-mesons seem to originate mainly from the decay of the pi-meson, since there is, as yet, no evidence for the direct production of mu-mesons in the nuclear interactions. The secondary mesons, are of course, charged, having the same charge as the parent pi-meson. They have a mass of 207 electron masses (45) and a lifetime of $2.1 \cdot 10^{-6}$ seconds (46) decaying into an electron plus two neutrinos (47). The spin of the mu-meson is $\frac{1}{2}$ (48). As already noted the mu-mesons are very penetrating because of their relatively weak interaction with matter.

The earlier phenomenological distinction between the hard and soft components (page 4) by reference to the thickness of lead they can penetrate can now be analyzed further. The former hard radiation is now seen to consist of a mesonic and nucleonic component, while the soft component, on the contrary, is formed by a preponderance of photons and electrons with a smaller fraction of low energy mesons and slow protons.

As the components diffuse through the atmosphere from the point of origin their composition will change. The particle intensity of the electron-photon component produced by the neutral pi-meson decay increases at first

by an alternating succession of radiative collisions and pair productions until the mean energy falls below the threshold for these processes and the component is absorbed. This roughly happens at an altitude of about 2 kilometers. For altitudes lower than this the soft component originates predominantly as a secondary effect of mu-mesons through electromagnetic collisions with atomic electrons and radiative collisions with nuclei as well as decay electrons. Thus for low altitudes the soft component is in equilibrium with the hard component and decreases with height approximately as does the generating component.

The particle intensity of the hard component, on the other hand, will decrease uniformly with distance from the producing layer and the absorption will be much smaller than for the soft component. The chief mechanism of disappearance of this component will be through mu-meson decay and therefore because of the relativistic time dilation the majority of the high energy mu-mesons will reach sea level.

The most striking phenomenon occurring in cosmic rays are extensive air showers or Auger showers, so named because the initial investigations were carried out by Auger and his collaborators (49). It has been established that these showers extend over many hundreds of meters, contain an extremely large number of electrons

and photons and a smaller percentage of charged-penetrating particles, and in all represent a very large energy release of the order of 10^{15} ev. Events of this type represent the collisions of the most energetic protons and heavy nuclei of the primary cosmic radiation with air nuclei. The soft component of the shower is the electron-photon cascade of the decay gamma rays of the neutral pi-mesons produced in the initial nuclear explosion at the top of the atmosphere, and the penetrating component is the result of a nucleonic cascade of the charged pi-mesons and nucleons produced in the same event.

The general phenomenological picture of cosmic radiation as described above is considered as fairly well established. However, further experimentation is required for confirmation and for a more detailed knowledge of the various events that take place. But any changes in the picture are expected to be only of secondary importance.

CHAPTER 2

ON ANOMALIES IN THE ABSORPTION OF COSMIC RAYS IN LEAD

The basic study of any radiation is that of its absorption in various materials. Thus, the absorption of cosmic rays in lead has been the subject of study by many workers during the past half-century. At the time that cosmic ray studies were first begun at this laboratory the general shape of the absorption curve was not in doubt, but some observers (50, 51, 52, 53, 54, 55, 56) had reported anomalies in the curve. It was, therefore, decided that before making use of the cosmic radiation as a source of mesons an investigation of any anomalies in the absorption should be made, even though the preliminary results of Heyland and Duncanson (57) indicated that no anomalies existed. During the course of investigation of the effect of lead above the telescope an anomalous increase in the counting rate was observed at a thickness of 12.5 cm. of absorber (58).

The reality of any such anomaly as the above was very seriously questioned after publication of detailed results by Heyland and Duncanson (59) which were confirmed independently by W. L. Kennedy (60). These investigators have searched specifically for anomalies and have failed to find any indication of the existence of such an anomaly

or any others. Hence, when a second telescope was built in 1952-53 the study of absorption in lead was repeated with a two-fold purpose. Firstly, it was an excellent way to test the operation of the equipment and secondly, it might provide more satisfactory results as to the existence of the anomalous maximum previously observed. As it turned out the present work corroborates the very careful measurements of Heyland and Duncanson.

Since the absorption experiment is of secondary interest and has been published in the literature a detailed account will not be given. However a reprint of the publication is contained in the Appendix. Figure 1 (page 113) shows the absorption curves for both the initial experiment (curve I) and the later experiment (curve II). Curve I exhibits the previously mentioned anomaly while curve II shows no evidence of any anomalies to within 1% accuracy for thicknesses of lead up to 45 cm.

The telescope arrangements used for the absorption investigations are also shown in the inset of Fig. 1. The reader is referred to section 3.2 for further details on the counters and electronics.

CHAPTER 3

PRODUCTION OF KNOCK-ON SECONDARIES BY COSMIC RAY PENETRATING PARTICLES

3.1 A Statement of the Problem

As has been indicated in the General Introduction the electron component of cosmic rays at sea level originates predominantly as a secondary effect of the penetrating component. Since both meson decay and close collision electrons, i.e., atomic electrons knocked-on by the penetrating particles, are major sources of secondaries, it is of importance to study one or the other individually in order to determine their relative contributions. Decay electrons can be practically eliminated by observing the secondaries under dense materials.

Therefore, with this view in mind, many of the experiments on knock-on secondaries were for the purpose of determining the average number of electrons in equilibrium with the mesons emerging from dense materials (61, 62, 63). Other experimenters have investigated the characteristics of the knock-ons emerging from fixed thicknesses of various materials. Such properties as the integral energy spectrum (64, 65, 66) and angular distribution of the secondaries (67, 68) as well as their production in successive layers of material (69) have all been studied previously for fixed thicknesses of material.

The purpose of the present experiment is to investigate the relation between the number of knock-on secondaries excited in aluminum layers and the thickness of the layers.

It was originally intended to select a narrow band of meson energies by the anticoincidence method using cosmic radiation as the source and to do a series of observations for various meson energy ranges. It was hoped that this would contribute to the better understanding of the properties of the mu-meson as an elementary particle. Unfortunately this was found to be impractical because of the low counting rates. So it was decided to use the complete meson spectrum with a minimum cut-off energy determined by imposing a minimum range in lead.

This type of investigation has been carried out previously for various materials in which the knock-on is produced (70, 71, 72, 73). The general form of the variation in the number of knock-on secondaries as a function of the thickness of the material in which they are produced, as obtained by the various workers is in agreement except for the curve of van Pittius and van Heereden. The curves showing the variation can not be expected to be identical since the exact shape of a curve depends on the conditions of the experiment. Such things as the geometry of the telescope, the value of the minimum energy of the meson accepted by the apparatus, and the energy required for the knock-on to be detected

would effect the shape of the curve. Since it is not known to what extent the various factors would alter the apparent form of the variation a complete comparison between the various results can not be made (the early work is discussed further in section 3.7).

The present experiment was designed for a twofold purpose, firstly to test the correctness of the theoretical expression for the collision probability between mu-mesons and electrons, and secondly, to determine if the above mentioned factors could account for the discrepancies between the previously determined curves.

With this premise in mind aluminum was chosen as the material. This choice simplifies the theoretical calculations since the range-energy relation for electrons passing through aluminum is of a relatively well established simple form (74) even at appreciable thicknesses (of the order of 10 gm.-cm.$^{-2}$). This allows the calculation of an expected curve for the particular conditions and a comparison to be made with the experimental points.

The experimental observations, by themselves, can only be interpreted as the production of secondaries by the penetrating component of cosmic radiation, since the simple apparatus does not positively establish the identity of the particles detected. The interpretation of the phenomenon observed as being the ejection of knock-on

electrons from the material by mesons can only be arrived at by indirect arguments relying on previously determined experimental facts.

In the sections that follow, a discription of the apparatus, experimental and calculated results are given, as well as the justification for comparing the two sets of results.

3.2 Apparatus

(a) Geiger-Müller Tubes

The counters employed in this experiment are of the external cathode type (75, 75A). The mechanical construction of the tubes is shown in Figure 2. The soft glass envelope has a diameter of 1.5 inches and a wall thickness of 0.037 inches. The aquadag coating on the outside, being electrically conducting, forms the cathode and is kept at ground potential. The axial tungsten anode wire is 0.004 inches in diameter and has an active length of 20 inches. A positive potential is applied to the anode wire to produce the required electric field.

The glass used for the envelopes was reclaimed fluorescent light tubing. After opening and washing thoroughly with water, the tubing was cleansed with a strong acid solution and rinsed with distilled water. Then, following the glass blowing, the envelope was cleansed and rinsed a second time. The tungsten wire was flashed in a flame before insertion and was mounted under

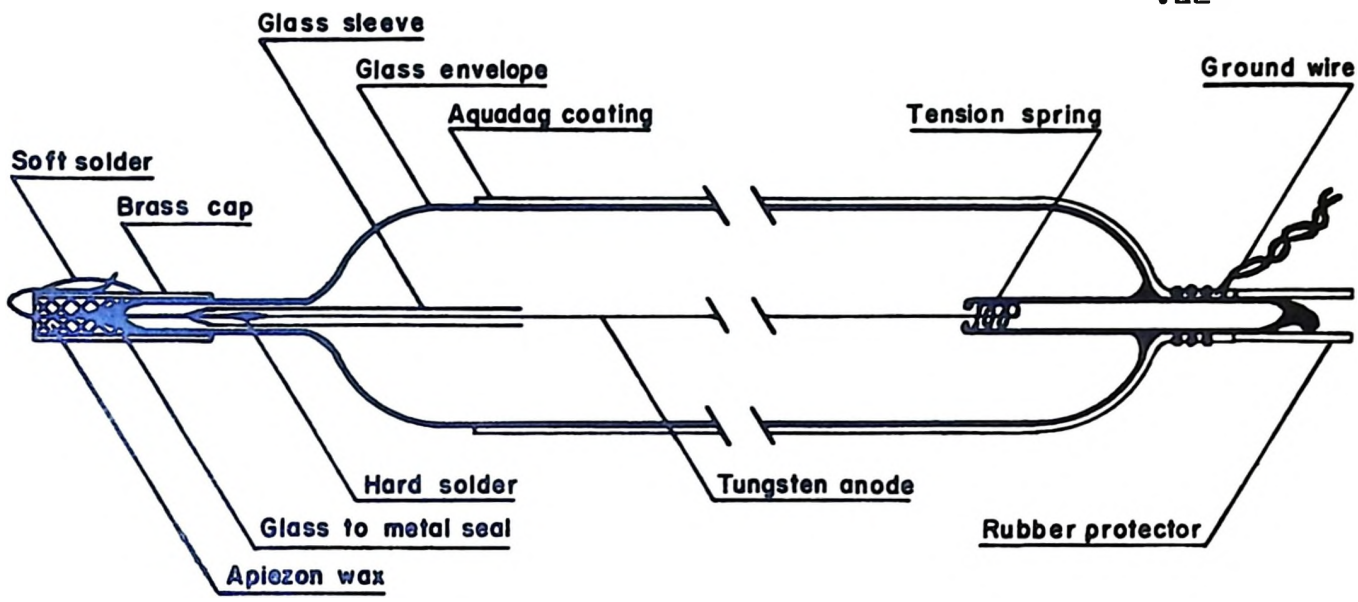

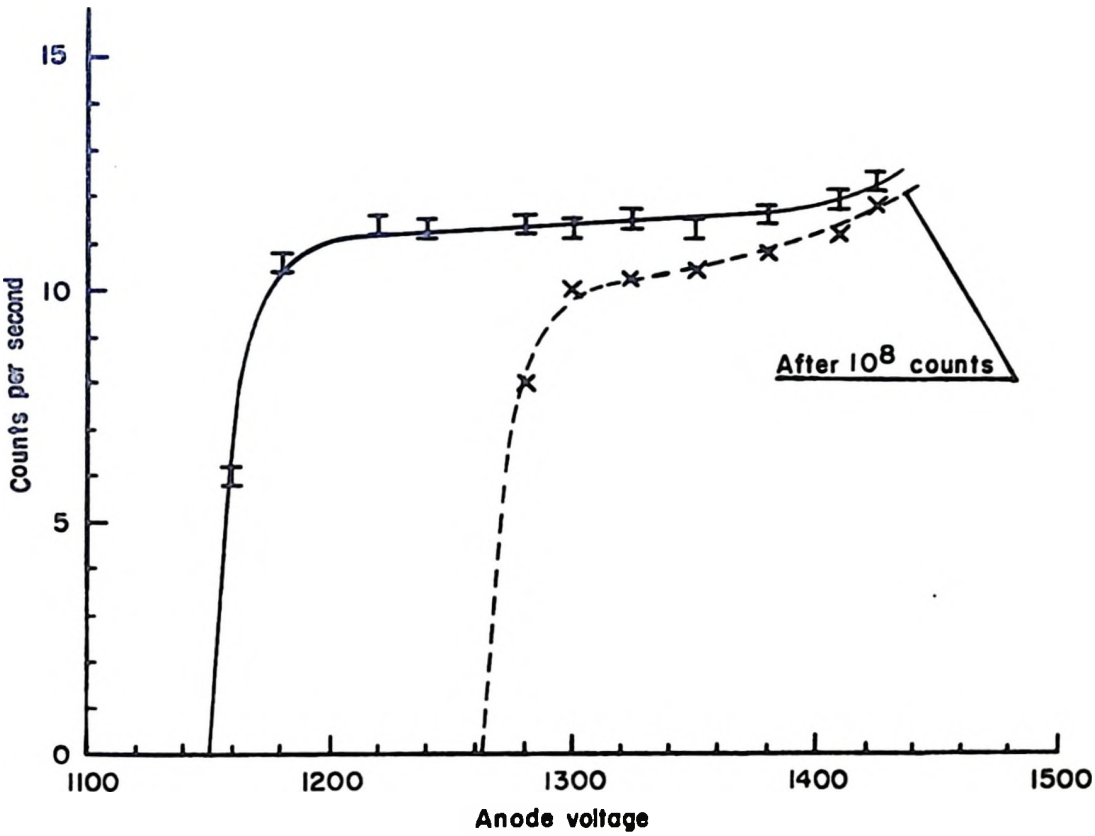

FIG. 2. Counter construction & characteristics

tension, by means of a spring, to prevent sagging.

Next, six tubes at a time were sealed onto the filling line manifold, and were out-gassed by baking at 150°C. while being evacuated for about four hours. The tubes were then filled to a pressure of 10 cm. of Hg., with 9 parts by volume argon and 1 part by volume ethyl formate. The use of ethyl formate as a quenching agent yielded better characteristics than the usual ethyl alcohol, the plateaus being both longer and flatter. (76) A typical plateau is shown in Figure 2.

After filling and sealing off from the filling line, the counters were cleaned and the coating of aquadag was sprayed on the outside. Also, since it was found that the counters became photosensitive after a short period of operation, a coating of black enamel was sprayed on to completely cover the tube, thereby protecting it from the light.

An acceptable tube was one which had a plateau characteristic longer than 125 volts with a slope less than 0.05% per volt. However, about 50% had slopes less than 0.02% per volt and about 50% had plateaus greater than 200 volts. With this criterion the rejects amounted to roughly 15%

It was found that, after filling, a counter required shelf aging of about one hour before the true counting action began. The characteristics seemed to

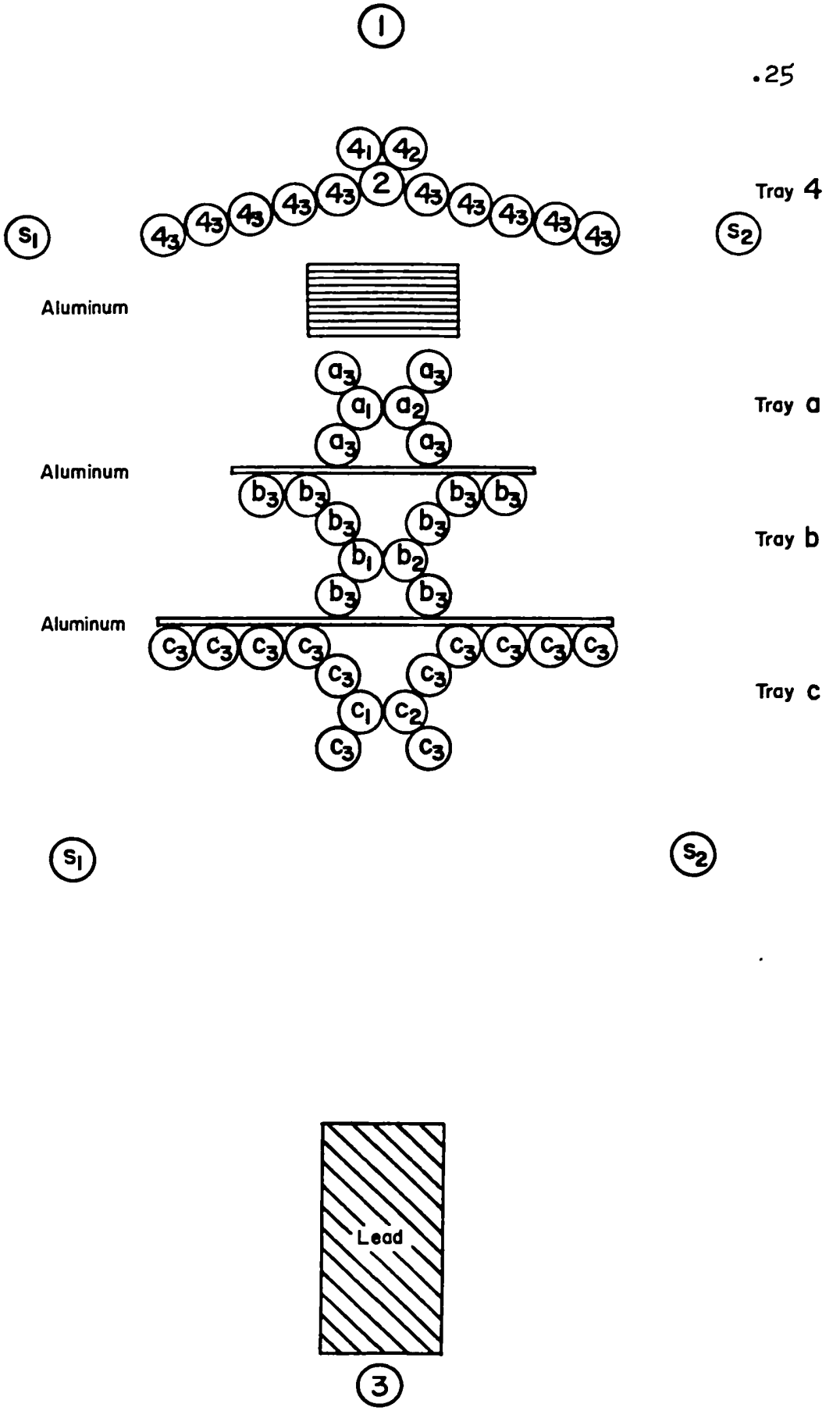

FIG. 3. Telescope configuration

are isolated from the rest and from each other. The third output from each tray is made up of the outside counters of that tray (i.e., those with suffix 3) in parallel. The shower detector consisted of 4 tubes but only two outputs. The tubes with the same designation (i.e., either s_1 or s_2) have a common output.

(c) Associated Electronics

The electronics are of conventional design and detailed circuit diagrams need not be given. A block diagram, however, is given in Figure 4. Each unit was built on a separate flat chassis and mounted vertically in a rack for ease in circuit alterations for a particular problem. The cathode followers and mixers marked 4 and a, b, and c, for the various counter outputs were mounted on the telescope rack as close as possible to the tubes. This permitted the use of short connecting leads thereby minimizing the capacitance in parallel with the counters. Also the cathode follower characteristics allow the use of coaxial shielded cable leads to the electronics rack without an appreciable increase in risetime of the pulses.

The three outputs from each of the four trays are fed into the correspondingly designated mixer. The requirement for these mixers to yield an output pulse is the simultaneous arrival of at least two input pulses. Hence the output pulses of mixer 4 are the coincidences $4_1 4_2$,

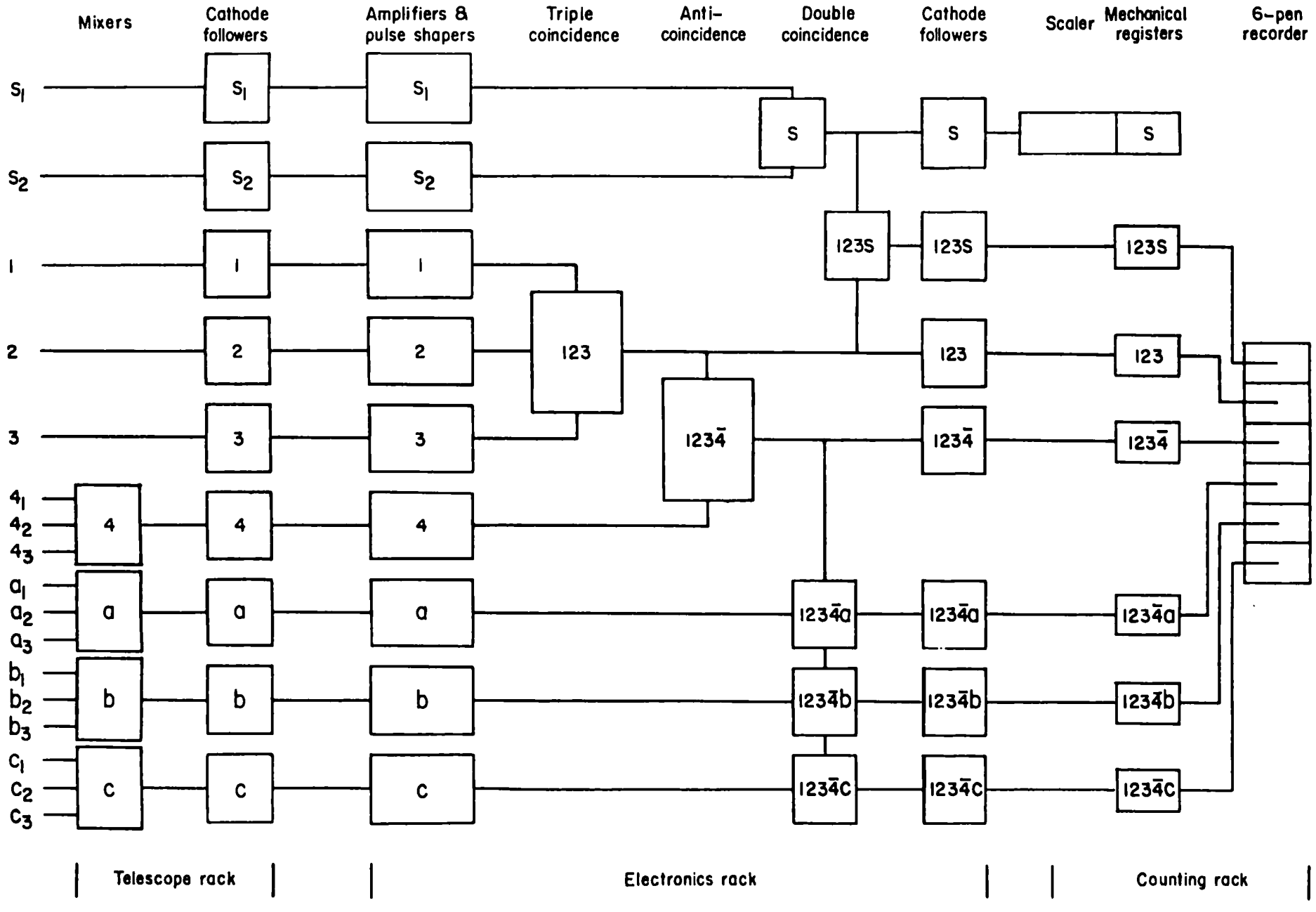

FIG. 4. Associated electronics

$4_1\bar{4}3$, $4\bar{2}43$, and $4_1\bar{4}2\bar{4}3$; the output pulses of mixer a are the coincidences a_1a_2, a_1a_3, a_2a_3, and $a_1a_2a_3$, and so on for the b and c mixers. The outputs of the four mixers will simply be designated correspondingly as 4, a, b, and c.

The various output pulses are then coupled to the electronics rack where they are amplified and sharpened to give a 2.5 microsec. triggering pulse for the pulse shapers. The pulse shapers yield uniform pulses 7.5 microsec. wide and either 85 volts positive or 140 volts negative. These pulses are combined in various coincident and anticoincident arrangements to yield outputs that can be interpreted as representing the physical phenomenon under study.

The resulting pulses are then fed through cathode followers and coaxial cables to the counting rack where they activate a Northern Electric Message Register ST5U and a corresponding pen on a 6 pen Esterline-Angus Operational Recorder and are thereby recorded.

The aperture of the telescope is defined by the 123 coincidence. These 123 counts give the number of particles traversing the telescope with sufficient energy to penetrate the 20 cm. of lead above counter 3.

In traversing the telescope the penetrating particle producing a 123 count will also trigger one of the inner counters of the four trays 4, a, b, and c.

If at the same time one or more other particles trigger the other inner counter or one of the outer counters of one or more of the trays, the mixer corresponding to the tray in which this happens will yield an output pulse. Thus this gives rise to the 4, a, b, and c pulses.

The 4 pulses are fed in anticoincidence with the 123 coincidence pulse. Hence if a second counter is fired in tray 4 simultaneously with the passage of the penetrating particle, the anticoincidence mixer will not yield an output pulse and no $123\bar{4}$ count will be registered. The $123\bar{4}$ counts are therefore interpreted as single penetrating particles, since there is no count if one or more accompanying particles are incident on the telescope.

Any a, b, or c pulses are fed into a set of mixers that are gated by the $123\bar{4}$ pulses. The outputs of these mixers give the counts $123\bar{4}a$, $123\bar{4}b$, and $123\bar{4}c$. These counts register the number of single penetrating particles that, upon traversing the telescope, produce a secondary particle in the material between trays 4 and a, 4 and b, 4 and c respectively.

Further information about any secondaries produced in the material between trays 4 and c may be gathered by analyzing the record chart. The chart is examined for the simultaneous registration of the $123\bar{4}a$, $123\bar{4}b$ and $123\bar{4}c$ pulses thereby determining if more than one tray was triggered by the same secondary and if so which trays.

One type of natural phenomenon which could give rise to a compound coincidence as recorded by this telescope is an air shower. This would then be interpreted incorrectly as a penetrating particle producing a secondary. Hence a shower detector was used to measure the magnitude of this effect. A shower is detected by the simultaneous firing of an s_1 and s_2 counter, i.e., an s coincidence. The s coincidences are recorded directly and also in coincidence with the 123 pulse. The 123s coincidences are also recorded on the chart.

3.3 The Experimental Procedure and Observations

Before the experiment proper was begun, a series of preliminary tests were performed, to insure that the apparatus was working properly. Spurious counts produced by the electronics or from external pick-up were tested for by simply lowering the counter high tension below threshold. No counts were recorded in a period of 72 hours. Also feed-through and cross-over between the various channels and mixers were tested for by monitoring the outputs without the required inputs. It was found that the outputs of the inner counters of each tray had to be well shielded electrostatically from each other and from the outer ones in that tray and that electrostatic shields had to be placed between the trays. However, when this was done there were no counts within 24 hours

without the required input pulses. In order to insure that the equipment continued to operate correctly, these tests were repeated from time to time during the course of the experiment. The negative results from the above tests are considered as adequate proof that, the counts registered during the experiment represent the required coincidences between the various pulses. In addition, to check the deterioration of the counter characteristics, their threshold potentials and single counting rates were monitored periodically.

When the telescope operated correctly the experiment proper was begun. The material used for the production of the secondaries consists of aluminum plates 0.823 gm.-cm.$^{-2}$ thick. Readings were taken for 15 different arrangements of the aluminum within the telescope, designated as follows: arrangement I, no aluminum in the telescope; arrangement II, one plate between trays b and c, only; arrangement III, one plate is placed between trays a and b keeping the plate between trays b and c. Then a plate is placed directly above tray a for each new arrangement until arrangement XIII has 10 plates above tray a, and one plate in each of the positions between trays a and b and trays b and c. Arrangements XIV and XV are similar to arrangement XIII except that arrangement XIV has 12 plates above tray a and XV has 15 plates above

tray a.

A reading for any given arrangement consisted of the number of counts registered in a period of approximately 24 hours, after which the arrangement was altered. The arrangements were not altered in any specified order. The reason for varying the thickness of aluminum within the telescope randomly is to prevent any regular variation in the number of counts registered caused by changes in experimental conditions being interpreted as dependent upon the thickness of material. Two such factors that could alter the counting rates uniformly are changes in detection sensitivity of either the counters or electronics and any regular atmospheric changes. Readings were taken until there were at least four sets of results for each arrangement.

Besides the readings yielded by the mechanical registers, a complete observation also includes the information obtained from the analysis of the chart. The simultaneous registration of pulses on the chart in different combinations define different types of events designated as follows: (the pulses 123 and $123\bar{4}$ will, of course, be simultaneous in each of the following cases)

Type of Event	Pulses Coincident
A	$123\overline{\Gamma}a$
B	$123\overline{\Gamma}b$
C	$123\overline{\Gamma}c$
AB	$123\overline{\Gamma}a + 123\overline{\Gamma}b$
AC	$123\overline{\Gamma}a + 123\overline{\Gamma}c$
BC	$123\overline{\Gamma}b + 123\overline{\Gamma}c$
ABC	$123\overline{\Gamma}a + 123\overline{\Gamma}b + 123\overline{\Gamma}c$

In addition to obtaining results for the arrangements designated above, readings for some secondary arrangements were also taken.

Firstly, since there is a possibility of the production of secondary particles in the walls of counter number 2 which could be detected by the trays, results were obtained for arrangements I and III with counter number 2 removed. These arrangements will be designated as I' and III'.

Secondly, in order to examine any possibility that the production of the secondaries depends on the material in which they are produced, 10.1 gm.-cm.$^{-2}$ lead, 10.7 gm.-cm.$^{-2}$ carbon and 10.0 gm.-cm.$^{-2}$ iron in turn were substituted in place of the aluminum above tray a.

Thirdly, in order to estimate the contribution to the counting rate due to side showers, the shower counts were recorded simultaneously with some of the readings obtained for arrangements III, VI, IX, XIII, and XIV and those when the iron, carbon and lead replaced the aluminum.

The total counts observed for the different arrangements of material in the telescope are given in Table I along with the respective times of observation. The shower results are set forth separately in Table II. The various number of events listed in this table are those which appeared to be concurrent with a shower, as determined from the chart analysis.

3.4 Correction and Interpretation of Results

Before the observations set forth in the tables can be interpreted as representing physical events, corrections for accidental counts must be made. The accidentals are of two types. Firstly, time accidentals are casually related pulses caused by two or more independent particles traversing the telescope within the resolving time of the electronics in such a way that a count is registered. Secondly, space accidentals are causally related events, where two or more related particles, other than the desired secondaries, traverse the telescope in such a way as to produce a count. These corrections are considered in more detail in the following sub-sections.

It is perhaps advisable to consider the question of errors before discussing the various corrections and the analyses of the results. In general, any uncertainty attributed to a numerical result is the usual standard

TABLE I

Total counts recorded and hours of observation.

	Time hrs.	123	123$\overline{4}$	123-123$\overline{4}$	123$\overline{4}$a	123$\overline{4}$b	123$\overline{4}$c	A	B	C	AB	AC	BC	ABC
I	128.69	5782	5091	691	216	400	521	65	115	261	32	7	141	112
II	116.36	5399	4651	748	196	395	507	56	121	274	52	11	145	77
III	178.75	8037	7116	921	297	610	754	131	229	425	65	13	228	88
IV	111.18	5163	4517	646	238	408	472	118	148	251	46	7	147	67
V	100.4	4561	4003	558	224	340	478	102	97	261	37	11	132	74
VI	175.18	8037	7053	984	464	664	830	215	207	428	80	25	233	144
VII	103.83	4743	4134	609	277	398	474	134	135	247	44	8	128	91
VIII	116.52	5235	4599	636	322	468	550	145	151	287	65	14	151	98
IX	169.56	7785	6942	843	513	726	808	223	222	372	93	25	239	172
X	102.67	4645	4073	584	300	386	492	137	101	245	48	10	132	105
XI	99.67	4408	3818	590	304	415	456	120	124	211	59	13	127	105
XII	235.68	10852	9392	1460	691	933	1137	312	279	569	109	23	298	247
XIII	117.94	5366	4626	740	358	482	565	162	148	268	55	18	156	123
XIV	180.47	8416	7338	1078	564	741	923	253	220	474	91	19	229	201
XV	146.68	6468	3708	760	472	630	724	194	184	346	82	14	182	182
I'	131.20	6716	5852	864	147	421	574	51	127	279	15	16	214	65
III'	101.56	5306	4603	703	107	333	491	43	115	273	7	7	161	50
C	104.32	4830	4207	623	332	441	541	154	124	252	46	21	160	111
Fe	100.18	4644	4070	574	295	380	429	144	125	206	46	14	118	91
Pb	119.76	5393	4724	669	280	417	514	106	122	255	46	10	131	118

TABLE II

Total results observed with the shower configuration.

	Time hrs.	123	123$\bar{4}$	123s	123$\bar{4}$s	As	Bs	Cs	ABs	ACs	BCs	ABCs	s
III	54.99	2490	2172	98	5						1	10	9499
VI	43.00	1955	1761	73	4				1	1		11	6961
IX	71.39	3237	2881	131	6		1		1			9	12592
XII	64.83	2564	2941	112	6							8	11134
XIV	74.60	3451	3000	139	14			1	1			6	13315
C	104.32	4830	4207	196	14	1				1	1	12	18265
Fe	97.48	4644	4070	181	16							7	17622
Pb	119.76	5393	4724	237	24		1	1	2		4	18	21134

deviation assuming that the cosmic ray events are independent and take place at random, and therefore, follow a Poisson distribution (see sub-section (a) below). Thus the standard deviation is given by $\bar{n}^{\frac{1}{2}}$ (77) where $\bar{n}$ is the average number of events recorded in an observation whether it be counts per hour or events per thousand incident particles. Furthermore, if several observations are taken the standard deviation is reduced in proportion to the inverse of the square root of the number of observations (78).

In the sections that follow the errors are not shown in the various tables in order that they should not become unnecessarily cumbersome. However, the errors are stated whenever a specific reference is made to a result and when the results are shown in graphical form.

(a) Chart Corrections

The apparent number of events observed on the chart will be different from the true number of events of a given type because of the finite probability of two gating pulses arriving within a time interval such that they are not resolved by the chart speed. When this happens the two pen marks will fall one on the other, and if one penetrating particle producing the $123\overline{\Pi}$ count should give rise to an A event and the other penetrating particle give rise to a B event, this would appear as an AB event on the chart. Other types of false events

would also appear on the chart through the various possible combinations of true events that could be produced by the two penetrating particles.

It is customary to assume that the particles incident on the telescope are random in time and follow a Poisson distribution given by

$$P(n) = \frac{(\bar{n})^n e^{-\bar{n}}}{n!}$$

where $P(n)$ is the probability of observing n particles in a given time interval if the average number of particles observed in the time interval is $\bar{n}$.

The probability that the interval between two successive particles is greater than t is equal to the probability $P(o)$ that no particle will occur in the time t. The average number of counts in the time t is equal to the product r, the average rate of passage of particles through the telescope times the time t. Thus $\bar{n} = rt$ and $P(o) = e^{-rt}$. Therefore the probability that two or more rays pass through the telescope within the time interval t is $p = 1 - e^{-rt}$.

A realistic value of the time t for this consideration is the time equivalent of the width of the pen mark, namely 1/60 of an inch. Thus if the chart speed is x inches per hour then $t = 1/60x$ hours. And if the total running time of the chart is T, and the number of gating pulses observed is N, then $r = N/T$. Thus

$rt = N/60xT$. Therefore the probability of the pen strokes of two or more gating pulses appearing as a single mark is $p = 1 - \exp.(-N/60xT)$. The number of cases in which this situation will arise during the observation of N gating pulse will be Np. In what follows the cases of more than two pulses being unresolvable can be neglected since their contribution is less than 3% of the total number of cases.

If the numbers of events of type A, B, C, AB, etc., that are actually produced by the N penetrating particles are A_T, B_T, C_T, AB_T, etc., then the probabilities of production of the various events are A_T/N, B_T/N, C_T/N, AB_T/N, etc.

Thus of the Np cases in which two pulses appear as one, the probability that one of the particles produces an A event is $pN\,(A_T/N) = pA_T$ and the probability that the other one produces a B event $= (p/N)\,A_TB_T$. This gives the number of events that are apparent AB events but are actually separate A and B events.

$$(AB)_a = (p/N)\,A_TB_T$$

By a similar argument the other compound events that are actually separate events are

$AC_a = (p/N)\,A_TC_T$

$BC_a = (p/N)\,B_TC_T$

$ABC_a = (p/N)\,(AB_TC_T + AC_TB_T + A_TBC_T)$

Hence the true number of events associated with N single penetrating particles are related to the observed number, designated by the suffix o, by the following

$$A_T = \frac{A_o}{1-(p/N)\ (B_T + BC_T + C_T)}$$

$$B_T = \frac{A_o}{1-(p/N)\ (A_T + AC_T + C_T)}$$

$$C_T = \frac{A_o}{1-(p/N)\ (A_T + AB_T + B_T)}$$

$$AB_T = \frac{AB_o-(p/N)\ A_TB_T}{1-(p/N)\ C_T}$$

$$AC_T = \frac{AC_o-(p/N)\ A_TC_T}{1-(p/N)\ B_T}$$

$$ABC_T = ABC_o-(p/N)\ (AB_TC_T + AC_TB_T + A_TBC_T)$$

Substituting the known values of x, N, T into these equations the true number of events can be determined by successive calculations. That is, substituting the observed values into the right hand side of the equation for A_T, a value for A_T can be determined. Then using this value along with the observed values for the other factors a value for B_T can be obtained and so on for the other equations. Then the process can be repeated using the calculated values. However, the

corrections are small enough so that one calculation is sufficiently accurate.

(b) Correction for Penetrating Particle Detection Inefficiency

Since the tray mixers require a double coincidence to yield an output, the penetrating particle producing the secondary that is detected by the tray must trigger one of the inner counters of the tray to yield the second pulse required for the coincidence. Thus any secondaries which are created by a penetrating particle that fails to activate one of the inner counters of a tray or passes between them will not be detected by that tray. The magnitude of this effect can be determined by feeding the single pulses from the inner counters of the various trays in coincidence with the gating pulse. The results obtained are as follows:

Time	123	1234	$\overline{A}$	$\overline{B}$	$\overline{C}$	$\overline{AB}$	$\overline{AC}$	$\overline{BC}$	$\overline{ABC}$
51.33 hr.	2352	2056	102	116	100	33	2	37	41

where $\overline{A}$ is the number of cases in which only the a tray is not fired; $\overline{AB}$ the number of times both the a and b trays (but not the c) are not fired; $\overline{ABC}$ the number of times that the a, b, and c trays are all missed by the penetrating particle and so on.

Thus for example the probability that the secondary producing particle fails to fire the a tray only is $\overline{P}_A = \overline{A}/1234 = 0.050$. The values for the various probabilities

are

$\overline{P}_A$	$\overline{P}_B$	$\overline{P}_C$	$\overline{P}_{AB}$	$\overline{P}_{AC}$	$\overline{P}_{BC}$	$\overline{P}_{ABC}$	$\overline{P}_a$	$\overline{P}_b$	$\overline{P}_c$
0.050	0.056	0.049	0.016	0.001	0.013	0.020	0.087	0.110	0.088

The observed values with suffix o are related to the true values with no suffix by the following equations.

$A_o = A + (\overline{P}_B + \overline{P}_{BC})\ AB + \overline{P}_{BC}\ ABC + (\overline{P}_C + \overline{P}_{BC})\ AC - \overline{P}_a A$

$B_o = B + (\overline{P}_A + \overline{P}_{AC})\ AB + \overline{P}_{AC}\ ABC + (\overline{P}_C + \overline{P}_{AC})\ BC - \overline{P}_b B$

$C_o = C + (\overline{P}_B + \overline{P}_{AB})\ BC + (\overline{P}_A + \overline{P}_{AB})\ AC + \overline{P}_{AB}\ ABC - \overline{P}_c C$

$AB_o = AB + \overline{P}_C\ ABC - (\overline{P}_A + \overline{P}_{AC} + \overline{P}_B + \overline{P}_{BC} + \overline{P}_{AB} + \overline{P}_{ABC})\ AB$

$AC_o = AC + \overline{P}_B\ ABC - (\overline{P}_A + \overline{P}_{AB} + \overline{P}_C + \overline{P}_{BC} + \overline{P}_{AC} + \overline{P}_{ABC})\ AC$

$BC_o = BC + \overline{P}_A\ ABC - (\overline{P}_B + \overline{P}_{AB} + \overline{P}_C + \overline{P}_{AC} + \overline{P}_{BC} + \overline{P}_{ABC})\ BC$

$ABC_o = ABC - (\overline{P}_A + \overline{P}_B + \overline{P}_C + \overline{P}_{AB} + \overline{P}_{AC} + \overline{P}_{BC} + \overline{P}_{ABC})\ ABC$

$a_o = a - \overline{P}_a a$

$b_o = b - \overline{P}_b b$

$c_o = c - \overline{P}_c c$

Substituting the numerical values for the probabilities the equations become:

$ABC = 1.266\ ABC_o$

$BC = (BC_o - 0.050\ ABC)\ 1.191$

$AC = (AC_o - 0.056\ ABC)\ 1.183$

$AB = (AB_o - 0.049\ ABC)\ 1.1925$

$A = (A_o - 0.074\ AB - 0.013\ ABC - 0.067\ AC)\ 1.096$

$B = (B_o - 0.051\ AB - 0.001\ ABC - 0.050\ BC)\ 1.124$

$C = (C_o - 0.072\ BC - 0.066\ AC - 0.016\ ABC)\ 1.097$

$a = 1.096\ a_o$

$b = 1.124\ b_o$

$c = 1.097\ c_o$

(c) Casual or Chance Coincidences

As pointed out previously some of the coincidences recorded will be due to two or more unrelated particles traversing the telescope within a time less than the resolving time in such a way as to produce a coincidence.

From general considerations (79) it can be shown that the accidental counts registered from n channels of pulse widths T_i and counting rates N_i is given by

$$A_n = N_1N_2....N_n(1/T_1 + 1/T_2 +....1/T_n)\ (T_1T_2....T_n)$$

If the T's are all the same value, then a twofold accidental is given by

$$A_{12} = 2\ N_1\ N_2\ T$$

The value of T in this experiment is reasonably constant and is equal to $7.5 \cdot 10^{-6}$ sec. Also since $T \ll 1$ and the counting rates are low any accidentals higher than twofold can be neglected. The formulae for the various accidental rates for the different coincidences are presented below. In each case the rates used are in counts per second and T is in seconds, yielding the accidentals in counts per hour.

(i) <u>123 coincidences</u>

$$A_{123} = [(N_{12} - N_{123})\ N_3 + (N_{23} - N_{123})\ N_1]2T\ 3600*$$

(ii) <u>123$\overline{4}$ anticoincidences</u>

$$A_{123\overline{4}} = [(N_{12\overline{4}} - N_{123\overline{4}})\ N_{3\overline{4}} + (N_{23\overline{4}} - N_{123\overline{4}})\ N_{1\overline{4}}]\ 2T\ 3600$$

* The term $(N_{13} - N_{123})\ N_2$ is neglected since it is ideally equal to zero ($N_{13} = N_{123}$) and experimentally very small.

(iii) $123\bar{4}a$ coincidences

There are many combinations of coincidences taken in pairs which can contribute to the $A_{123\bar{4}a}$ coincidence; however, the only important terms are

$$A_{123\bar{4}a} = (N_{12\bar{4}a}\, N_{3\bar{4}} + N_{123\bar{4}}\, N_{a\bar{4}})\ 2T\ 3600$$

The expression for the $A_{123\bar{4}b}$, $A_{123\bar{4}c}$, etc., accidentals are the same as for the a accidentals with the appropriate symbol (b, c, etc.) replacing the a in the above equation.

The expressions for the chance coincidences for the arrangements I' and III' with counter 2 removed are:

(iv) 13 coincidences

$$A_{13} = N_1\, N_3\ 2T\ 3600$$

(v) $13\bar{4}$ anticoincidence

$$A_{13\bar{4}} = (N_{1\bar{4}} - N_{13\bar{4}})\, N_{3\bar{4}}\ 2T\ 3600$$

(vi) $13\bar{4}a$ coincidence

$$A_{13\bar{4}a} = (N_{1\bar{4}a}\, N_{3\bar{4}} + N_{13\bar{4}}\, N_{a\bar{4}})\ 2T\ 3600$$

Again the expressions for the remaining accidental rates are the same as for the a ones with the appropriate substitution.

(d) Anticoincidence Inefficiency (Causal Accidentals)

The purpose of the anticoincidence tray is to select single penetrating particles and reject any that may have accompanying radiation. Any penetrating particles contained in an air shower will, of course, have accompanying

radiation. Other sources of particles that may traverse the telescope concurrently with the desired particle would be secondaries from local showers or knock-ons produced in the roof or in the telescope supports, which could pass through the telescope directly, or be scattered into it by the surrounding material. In addition two or more penetrating particles (hard showers) may traverse the telescope simultaneously giving rise to a false count.

If the accompanying radiation triggers tray 4 , the event would be cancelled. However, the anticoincidence tray is not 100% efficient. Any accompanying particle which is at an angle such as to pass through the same anticoincidence counter as the penetrating particle, or comes from the side or end such as to miss tray 4 would not be detected by the guard tray and the event would not be rejected. Besides the geometric inefficiency due to the fact that the anticoincidence tray does not protect the telescope from all angles, there is the inefficiency analogous to that of the other trays; namely the failure of the penetrating particle to trigger one of the inner counters and hence its failure to supply a second pulse for the mixer.

The efficiency for the triggering of an inner counter of tray 4 by the penetrating particle can be determined as in the case of the other trays. Except in this case the single pulses from the two inner counters

are fed in anticoincidence with the 123 coincidence pulse. Of 4000 penetrating particles traversing the telescope only 341 failed to trigger one of the inner counters of tray 4, thus the efficiency for detection is 91.5%.

Thus the number of penetrating particles with accompanying radiation given by the difference between the 123 - 123$\bar{4}$ counts is only 91.5% of the value it should be and, therefore, the true value is given by (123 - 123$\bar{4}$)/0.915. In order to correct the number of counts representing the various types of events for this anticoincidence inefficiency, the relative number of coincidences of the various types produced by the accompanying radiation must be known. To obtain this the coincidence 134 was used as the gating pulse. The results are given in Table III for the different arrangements of the aluminum, and those that are accompanied by a discharge of the shower detector are noted separately. There is no significant difference between the values obtained for different arrangements of materials so the results have been totalled in order to have better statistics.

After correcting for penetrating particle detection efficiency and accidentals, the relative intensities are obtained by normalizing 134 to unity. These values can now be used to correct the experimental observations.

TABLE III

Results used for anticoincidence inefficiency calculations.

	Time hrs.	134	A	B	C	AB	AC	BC	ABC	134 only	a	b	c
						Total events							
I	33.96	248	14	7	18	18	6	22	87	76			
III	33.52	200	7	8	8	14	6	16	76	65			
XV	33.71	236	12	11	11	19	4	11	76	92			
Total	101.19	684	33	26	37	51	16	49	239	233	339	355	341
						With showers							
I		63	2	2	2	3	3	5	45	1			
III		53	0	0	1	5	1	5	40	1			
XV		51	2	2	0	3	3	3	37	1			
Total		167	4	4	3	11	7	13	122	3			
						Totals corrected for penetrating particle detection inefficiency							
Total events		684	26.7	24.2	35.0	43.2	0	40.4	302.5	212			
With shower		167	1.0	3.7	0	4.1	0	6.3	154.5	0			
						Corrected for accidentals							
Total events		638.4	24.0	22.6	32.0	42.5	0	39.2	301.2	201.5	367.7	405.5	372.4
With shower		165.4	1.0	3.7	0	4.1	0	6.3	152.9	0			
						Fraction of accompanying radiation that produces various events							
		1.000	0.038	0.035	0.050	0.067	0	0.061	0.471	0.316	0.576	0.635	0.582

For example, it is now known that 57.6% of the accompanying radiation fires the a tray. The number of penetrating particles with accompanying radiation that fail to trigger the anticoincidence tray is

$$(123 - 123\overline{4})\,[(1/0.915) - 1]$$

and of these, the number that would produce an a event is

$$0.576\ (123 - 123\overline{4})\,[(1/0.915) - 1]$$

This number then should be subtracted from the a counts. The corrections for the other types of events are made in a similar manner.

Unfortunately the correction for the causal coincidences resulting from the situation first dealt with in this section, namely the accompanying radiation completely missing the anticoincidence tray, cannot readily be estimated. A discussion of this effect and other sources of causal coincidences will be reserved till later.

(e) Corrections for Compound Events

In passing through the material the penetrating particle has a finite probability of producing an A event, whether this be by producing a secondary in the material above tray a or being caused by an accompanying particle from outside the telescope. Let this be represented by P(A). Also there is a finite probability P(B) that

a B event will be produced. Hence there is a definite probability that both will be produced simultaneously given by $P(A) \cdot P(B)$. This compound A and B event would not be distinguishable from a true AB event. In a similar manner other combinations of the various types of events could give rise to compound events that would be incorrectly interpreted as representing single events. Hence corrections must be made for this effect. The formulae relating the true number of events to the observed number are given by (neglecting triple compound events).

$$P_o(A) = P_T(A) \left[1 - P_T(B) - P_T(BC) - P_T(C)\right]$$

$$P_o(B) = P_T(B) \left[1 - P_T(A) - P_T(C)\right]$$

$$P_o(C) = P_T(C) \left[1 - P_T(A) - P_T(B) - P_T(AB)\right]$$

$$P_o(AB) = P_T(AB) \left[1 - P_T(C) + P_T(A)\, P_T(B)\right]$$

$$P_o(AC) = P_T(A)\, P_T(C)$$

$$P_o(BC) = P_T(BC) \left[1 - P_T(A) - P_T(B)\, P_T(C)\right]$$

$$P_o(ABC) = P_T(ABC) + P_T(A)\, P_T(BC) + P_T(AB)\, P_T(C)$$

Where P_T represents the true probabilities of the production of an event and P_o the observed probabilities. The values for the true probabilities can now be determined by successive calculations as for the chart corrections.

(f) Correction of Shower Results

The number of $123\overline{4}$s pulses recorded during the times of observation of the showers is about the number that would be expected from casual coincidences of 123s and $123\overline{4}$ pen marks on the chart. Also, the number of

events other than ABC that are associated with a shower is about the number expected from the inefficiency of the penetrating particle to fire an inner counter of the various trays. Therefore, it is reasonable to assume that the $123\overline{4}s$ are actually 123s events, and in the cases where the anticoincidence tray is not fired, the other three trays are all fired. Thus the shower events are of two types, 123s and $123\overline{4}sABC$, the second type owing its existence to the failure of the penetrating particle to fire one of the inner counters of tray 4.

(g) Discussion and Interpretation

The corrections are applied to the totals of Table I in the order in which they have been presented. The end results of the analysis are given in Table IV. Although the corrections are many, the end results are very little different from the original observations as can be seen from a comparison of the two tables. The reason for this is that some of the corrections are positive while others are negative and upon successive application they tend to cancel each other giving only a small net effect.

The logical procedure now is to examine the results in detail for any variation that could be related with changes in the experimental conditions and to determine what physical phenomenon may be responsible.

From the hourly counting rates given in Table V

TABLE IV

The total number of events after corrections.

	Time hrs.	123	123$\bar{4}$	123-123$\bar{4}$	123$\bar{4}$a	123$\bar{4}$b	123$\bar{4}$c	A	B	C	AB	AC	BC	ABC
I	128.69	5755	5007	748	190	400	525	54.5	110.8	259.9	24.0	0	154.2	111.4
II	116.36	5375	4564	811	167	392	507	48.1	115.9	277.2	50.3	4.6	161.4	64.7
III	178.75	7999	7002	997	264	629	764	129.5	227.8	434.7	63.1	0.2	257.7	70.8
IV	111.18	5136	4440	696	219	413	475	121.4	147.2	256.4	43.2	1.9	165.2	56.5
V	100.4	4540	3936	604	209	342	487	105.4	91.7	269.9	34.9	0.1	147.3	69.1
VI	175.18	8000	6934	1066	444	677	843	223.9	211.1	442.7	76.6	4.0	259.1	139.0
VII	103.83	4722	4061	661	264	404	479	135.7	133.0	250.8	40.7	0	140.9	88.4
VIII	116.52	5210	4522	688	311	481	560	149.8	152.3	296.4	64.9	0	167.6	96.1
IX	169.56	7751	6837	914	505	755	818	230.6	218.4	378.9	90.8	3.0	265.0	180.4
X	102.67	4624	4004	620	291	393	501	138.4	95.9	248.2	44.6	0	144.9	107.7
XI	99.67	4387	3748	639	295	424	461	122.3	121.4	214.8	57.7	0	138.9	117.0
XII	235.68	10803	9219	1584	663	947	1150	314.2	275.3	576.2	99.7	0	325.4	248.5
XIII	117.94	5341	4540	801	345	491	571	169.4	145.5	275.2	50.5	1.4	170.9	123.3
XIV	180.47	8377	7210	1167	548	757	940	265.8	216.0	493.7	84.8	6.5	249.4	207.2
XV	146.68	6436	5618	818	467	654	742	191.5	182.5	346.8	77.7	0	197.1	197.0
I'	131.20	6152	5353	899	106	415	573	42.2	118.8	272.3	6.4	11.4	243.7	45.8
III'	101.56	4869	4136	733	73	327	493	35.8	108.8	272.4	4.0	0	182.8	33.6
C	104.32	4808	4135	673	324	453	570	162.7	119.9	258.5	41.6	3.7	177.6	113.4
Fe	100.48	4623	4001	622	285	387	454	150.7	129.1	211.2	43.5	1.5	129.3	90.1
Pb	119.76	5367	4643	724	263	422	533	102.3	118.7	256.8	40.6	0	142.0	120.1

TABLE V

The various counting rates in counts per hour; the fraction of penetrating particles accompanied by secondary radiation and showers, and the efficiency of shower rejection.

	123	$123\bar{4}$	$123-123\bar{4}$	$123\bar{4}a$	$123\bar{4}b$	$123\bar{4}c$	$\frac{123-123\bar{4}}{123}$	123s	s	$\frac{123s}{123}$	$\frac{123s-123\bar{4}sABC}{123s}$
I	44.7	38.9	5.8	1.5	3.1	4.1	0.130				
II	46.2	39.2	7.0	1.4	3.4	4.4	0.151				
III	44.8	39.2	5.6	1.5	3.5	4.3	0.125	1.78	172	0.039	90
IV	46.2	39.6	6.3	2.0	3.7	4.3	0.136				
V	45.2	39.2	6.0	2.1	3.4	4.9	0.133				
VI	45.7	39.6	6.1	2.5	3.9	4.8	0.133	1.70	161	0.038	88
VII	45.5	39.1	6.4	2.5	3.9	4.6	0.140				
VIII	44.7	38.8	5.9	2.7	4.1	4.8	0.133				
IX	45.7	40.3	5.4	3.0	4.4	4.8	0.118	1.83	175	0.040	92
X	45.0	39.0	6.0	2.8	3.8	4.9	0.134				
XI	44.0	37.6	6.4	3.0	4.3	4.6	0.146				
XII	45.9	39.2	6.7	2.8	4.0	4.9	0.147	1.73	171	0.042	94
XIII	45.3	38.5	6.8	2.9	4.2	4.8	0.150				
XIV	46.4	39.9	6.5	3.0	4.2	5.2	0.139	1.86	178	0.040	95
XV	43.9	38.3	5.6	3.2	4.5	5.1	0.127				
I'	46.9	40.8	6.8	0.8	3.2	4.4	0.146				
III'	48.0	40.7	7.2	0.7	3.2	4.8	0.150				
C	46.1	39.6	6.4	3.1	4.3	5.5	0.140	1.88	175	0.041	93
Fe	46.0	39.8	6.2	2.8	3.8	4.4	0.135	1.86	180	0.039	96
Pb	44.8	38.9	6.0	2.2	3.5	4.6	0.135	1.98	176	0.044	91

it is noted that the counting rates of the 123 and $123\overline{4}$ pulses are essentially constant for the different arrangements. The fluctuations that are present appear randomly and can readily be attributed to statistical fluctuations since the root mean square deviation of the numbers set forth in the table equals the statistical standard deviation. This is not true for the counting rate of the accompanying radiation as determined from the 123 - $123\overline{4}$ rates. In this case the root mean square deviation is about twice that expected if only counting statistics are considered. However, it is reasonable to attribute this larger fluctuation as being caused by changes in meteorological conditions which would have a larger effect on the accompanying soft radiation. Thus the ability of the telescope to detect particles incident upon it remained stable throughout the experiment.

The alignment of the coincidence counters can be checked from a comparison of the average rates with counter 2 in the telescope (normal configuration) and counter 2 removed (arrangements I' and III'). The results are given in Table VI.

TABLE VI

The counting rates required for checking the telescope alignment.

Coincidence	Counts per hour
123	45.4 ± 0.1
$123\overline{4}$	39.2 ± 0.1
13	47.4 ± 0.4
$13\overline{4}$	40.8 ± 0.4
123/13	0.96 ± 0.01
$123\overline{4}/13\overline{4}$	0.96 ± 0.01

The 123/13 ratio is expected to be less than unity because of three factors. Firstly, the two-counter arrangement is more efficient in detecting an ionizing particle than the three-counter one. If the efficiency of detection for a single counter is ϵ and the actual number of particles traversing the telescope is N, then the number recorded by the double coincidence would be $\epsilon^2 N$, and $\epsilon^3 N$ by the triple one. The ratio of the triple coincidence counting rate to the double would be ϵ. For a counter of the dimensions of the ones used in this experiment and filled to the same pressure the efficiency for detecting an ionizing particle is greater than 99.9%. Secondly, a decrease in the counting rate with the addition of a counter in coincidence would be expected from the finite dead time or insensitive period of the added counter. There is a finite probability that a

particle detected by counters 1 and 3 would pass through counter 2 while it was still below threshold potential following a discharge by a casual particle. The dead time of the counters used is of the order of $4 \cdot 10^{-4}$ seconds. This was determined by displaying the pulses of a counter on a slow triggered trace of an oscilloscope with a moderate counting rate. The natural counting rate of an individual counter is approximately 10 counts per second. Therefore, in a period of 1 second the counter is insensitive for $4 \cdot 10^{-3}$ seconds or 0.4% of the time. Thus the counting rate would be reduced by 0.4% with the addition of a counter in coincidence. Thirdly, if the counter 2 is not exactly in line with counters 1 and 3 then the restriction that the particle must fire counter 2 would prevent those whose paths did not pass through counter 2 from being detected.

The observed decrease in counting rate is 4%. Since the first two factors mentioned above are negligible, this difference must be attributed to a misalignment of the counters. Furthermore, since the ratio is the same for the anticoincidence channel as for the coincidence one, the displacement is essentially longitudinal rather than lateral.

An examination of the counting rates from the three lettered trays indicates an increase in counting rates with an increase in the thickness of material in the

telescope, particularly for the a tray. The question arises as to what phenomenon could be responsible for this increase.

It may well be due to the desired effect of the production of secondaries by the penetrating particles in passing through the material. On the other hand, before the increase can be ascribed to this phenomenon, all other possibilities must be discarded. The only other particles that could discharge a second counter in any of the trays, other than a secondary emerging from the material, are ones making up the accompanying radiation. The ratio $(123 - 123\overline{4})/123$, as determined in Table V, yields the value of $(13.6 \pm 0.2)\%$ for the average number of penetrating particles that are accompanied by secondary radiation which triggers tray 4 and $(4.0 \pm 0.05)\%$ is the average number that have accompanying radiation of sufficient density to cause a shower count as denoted by the ratio 123s/123.

Thus the anticoincidence tray rejects an appreciable number of the particles which have accompanying radiation, especially if the density is such as to cause a shower count. This latter fact can be seen by a comparison of the 123s counting rate of 1.84 ± 0.05 counts per hour (Table V) to the 134s counting rate of 1.73 ± 0.13 counts per hour (Table III). The ratio of these counting rates gives the value 94% for the efficiency of shower rejection

by the guard tray. A value for this efficiency is also determined by the ratio $(123s - 123\overline{4}sABC)/123s$ of Table V which has a mean value of 92%. Hence since only 4% of the penetrating particles are concurrent with large showers and of these 93% are rejected, the percentage of compound coincidences produced by showers is negligible.

However, if there are only a few accompanying particles and they should pass through the insensitive counter of the guard tray, or come from the side, then they could give rise to a count from the trays. Furthermore, they could be responsible for an increase in the counting rate if the efficiency for their detection was increased with the addition of material in the telescope. This effect is possible according to the following reasoning; if the accompanying particle is an electron that normally would not discharge a tray, then, with the insertion of the material, the electron could either initiate a shower in the material, which would cover a larger angle than the original single electron, or the original electron could be scattered into a path which would result in a discharge of a tray. If the accompanying particle is a photon it would have only a small chance of being detected no matter what its path because of the low efficiency of the counters in detecting uncharged particles. However, with the placing of material in the path of the photon, there is a finite

probability that the photon will "materialize" (i.e., create an electron-positron pair) and the charged particles produced would be readily detected by the counters. Both of these effects will increase with the thickness of material, thus an increase in counting rate would be expected.

If the increase in counting rate is in fact due to the accompanying radiation because of the effects described above, then the 10.1 gm.-cm.$^{-2}$ of lead should be much more effective than the 10.7 gm.-cm.$^{-2}$ of carbon. The results, on the other hand, give only an increase of 1.4 ± 0.2 counts per hour with lead over that with no material, while the carbon produces an additional 2.3 ± 0.2 counts per hour.

It is, therefore, reasonable to assume that the effect of the accompanying radiation is secondary and that the phenomenon which is chiefly responsible for the increase in counting rate is the only alternative one, namely production of secondaries in the material.

Following this supposition, the number of counts from the various channels per 1000 penetrating particles rather than counting rates will give a more realistic representation of any variation with change in arrangement. This will essentially eliminate any fluctuations which could arise from meterological changes, which would be manifested in the counting rates. The number of counts

per 1000 penetrating particles of the various coincidences are given in Table VII.

Continuing under the assumption that the phenomenon is the production of secondaries, then a tentative interpretation of the various coincidences in terms of physical events is possible as set forth below.

a, b, and c Events

These are interpreted as representing the production of a secondary in the material above trays a, b, and c, respectively.

A Event

This type of event represents the production of a secondary in the material above tray a but with insufficient energy to penetrate the material between trays a and b.

B Event

This event indicates the production of a secondary in the material between trays a and b, which does not have sufficient energy to penetrate the material between trays b and c.

C Event

A secondary produced in the material between trays b and c can only give rise to a C event.

AB Event

If a secondary created in the material above tray a has sufficient energy to penetrate the material between

TABLE VII

The number of the various types of events recorded per 1000 penetrating particles traversing the telescope.

	123$\bar{4}$a	123$\bar{4}$b	123$\bar{4}$c	A	B	C	AB	AC	BC	ABC	AB + ABC
I	38	80	105	11	22	52	5	0	31	22	27
II	36.5	86	111	10.5	25.5	60.5	11	1.0	35.5	14	25
III	37.5	90	109	18.5	32.5	62	9	0	37	10	19
IV	49.5	93	107	27.5	33	57.5	9.5	0.5	37	12.5	22.5
V	53	87	123.5	27	23.5	68.5	9	0	37.5	17.5	26.5
VI	64	97.5	121.5	32	30.5	64	11	0.5	37.5	20	31
VII	65	99.5	118	33.5	32.5	61.5	10	0	34.5	22	32
VIII	69	106.5	124	33	33.5	65.5	14.5	0	37	21	35.5
IX	74	110.5	119.5	33.5	32	55.5	13.5	0.5	39	26.5	39.5
X	75.5	98.5	125.5	34.5	24	62.5	11	0	36	27	38
XI	78.5	113	123	32.5	32.5	57.5	15.5	0	37	31	46.5
XII	72	102.5	125	34	30	62.5	11	0	35.5	27	38
XIII	76	108	126	37.5	32	60.5	11	0.5	37.5	27	38.5
XIV	76	105	130.5	37	30	68.5	12	1.0	34.5	29	40.5
XV	83	116.5	132	34	32.5	61.5	14	0	35	35	49
I'	20	77.5	105	8	22	51	1	2.0	45.5	8.5	9.75
III'	17.5	79	119	8.5	26.5	66	1	0	44	8	9.0
C	78.5	109.5	138	39.5	30	62.5	10	1.0	43	27.5	37.5
Fe	71.5	99.5	113.5	37.5	31	53	11	0.5	32.5	22.5	33.5
Pb	56.5	91	115	22	25.5	55.5	8.5	0	30.5	26	34.1

trays a and b but not enough to penetrate that between trays b and c, then an AB event will be recorded.

ABC Event

If a secondary emerges from the material above tray a with sufficient energy such that its range is greater then the combined thickness of material between trays a and b, and trays b and c, then it will produce an ABC event.

BC Event

An event of this type is manifested by the production of a secondary in the material between trays a and b which has sufficient energy to penetrate the material between trays b and c.

The events, AB, BC, and ABC, can, of course, in addition to the above ways, be caused by compound events as discussed previously. For example, the AB event could be caused by the simultaneous production of an A and B event. However, this effect has supposedly already been corrected for and should not be represented by the results contained in the table.

The results of Table VII seem to be in accord with the above interpretation as well as can be determined from the relatively poor statistics. The number of 123$\overline{4}$a, 123$\overline{4}$b, and 123$\overline{4}$c events, increase, on the whole, with increase in material above the trays. Also, in going from arrangement I to II (placing aluminum between trays b

and c) it would be expected that the number of A events would remain unchanged while the B, C, and AB events would increase, and the BC and ABC events would decrease, which is essentially the case. Then with the placing of aluminum between trays a and b (arrangement III), the number of A, B, and BC events should increase, the C events should remain the same, and the AB and ABC events should decrease. Then with each new arrangement the only events that should change are the a, b, c, A, AB, and ABC which should all increase with increasing arrangement number, which again is essentially borne out by the experiment.

The arrangements I' and III' should effectively represent the situation with no material above tray a, since even counter 2 is removed. There is, of course, still the anticoincidence tray and counter 1 in the telescope; however, a large number of the secondaries produced in the walls of these tubes would be eliminated by tray 4, thus the "effective" material thickness would be quite small and will be neglected. Nonetheless there is an appreciable number of events recorded for these arrangements. These counts will be treated as zero thickness background which could be due to the following causes.

Firstly, as already pointed out the geometric efficiency of the guard tray is not 100%, thus accompanying

radiation will produce some of the events. However, as already argued, there appears to be no major change in the number of events produced by this source with increase in the amount of material in the telescope.

Secondly, a misalignment of the 123 coincidence counters such that it becomes possible for a penetrating particle to traverse more than one counter of a given tray, would yield a constant number of outputs from the tray.

Thirdly, there is the possibility of production of secondaries in the lead above counter 3, that could be scattered back through the telescope. The number of counts produced by these particles would change with the addition of material between trays b and c and a and b, but should remain essentially constant thereafter.

Fourthly, some secondaries will be produced by the penetrating particles in the wall of the tray counter through which it passes. If the angle of ejection and the energy is such that the secondary can fire a second counter of the tray, a count will be registered. The number of secondaries produced in this manner will be independent of the thickness of material in the telescope.

Therefore, although there is an appreciable zero thickness count, it is essentially constant and can be treated as a background superimposed on the real events.

Because the events involving the a tray yield

the most information, and because the other events are more susceptible to background variations, only the secondaries produced in the material above the a tray will be treated completoly. These results are set forth separately in Table VIII where the thickness of material above the a tray includes the wall thicknesses of counter 2.

The number of $123\overline{4}a$ events represents the total number of secondaries emerging from the material above tray a which can activate a counter, normalized for 1000 incident particles. The AB + ABC events are produced by secondaries which have ranges greater than the thickness of material between tray a and b, namely, 1.31 gm.-cm.$^{-2}$, while the A events are produced by those whose ranges are less than this value. The ABC events are produced by those whose ranges are greater than the thickness of material between trays a and b and b and c, i.e., greater than 2.62 gm.-cm.$^{-2}$.

TABLE VIII

The different types of events involving the a tray and the thickness of material above that tray.

Thickness of material gm.-cm.$^{-2}$	Number of events per 1000 penetrating particles			
	$123\bar{4}a$*	A	AB + ABC	ABC
		Aluminum		
0	19	8.5	9	8
0.44	37.5	18.5	19	10
1.32	49.5	27.5	22.5	12.5
2.14	53	27	26.5	17.5
2.96	64	32	31	20
3.78	65	33.5	32	22
4.61	69	33	35.5	21
5.43	74	33.5	39.5	26.5
6.25	75.5	34.5	38	27
7.08	78.5	32.5	46.5	31
7.90	72	34	38	27
8.72	76	37.5	38.5	27
10.37	76	37	40.5	29
12.84	83	34	49	35
		Carbon		
11.2	78.5	39.5	37.5	27.5
		Iron		
10.5	71.5	37.5	33.5	22.5
		Lead		
10.1	56.5	22	34.1	26

* The discrepancies between the values of $123\bar{4}a$ and A + AB + ABC arise from approximations made during the process of correcting the original data, particularly those involving the AC events.

3.5 Nature of the Particles

The simple apparatus used for this experiment does not permit positive identification of the particles observed. However, from a consideration of other works, arguments can be presented as to the most probable nature of the particles and of the physical phenomenon under study.

(a) Penetrating Particles

As has already been noted, the penetrating component of the secondary radiation consists of mesonic and nucleonic constituents. Most of the nucleonic constituent at sea level is made up of neutrons (80). Any interactions produced by the neutrons in the material contained in the telescope would not be detected since the neutron would not have activated the entrance counters 1 and 2. The only effect neutrons could have would be the production of local penetrating showers through nucleon interactions in the roof above the apparatus which may or may not contribute to the causal accidentals. However, since the high energy neutron flux is estimated at about 6% of that of the ionizing penetrating radiation, and since the anticoincidence tray is reasonably effective in guarding against showers, the number of accidentals produced in this way would be negligible.

Any protons within the cosmic ray beam monitored by the telescope could produce the required coincidences,

either by giving rise to a penetrating shower in the aluminum or of a knock-on electron. The number of protons, with energy sufficient to penetrate the load above counter 3, make up less than 1% of the vertical cosmic ray intensity at sea level (81, 82); therefore, events produced by them will be a negligible percentage of the total.

Of the mesonic component at sea level, there has been fairly general agreement that the mu-mesons are very much more numerous than the pi-mesons. That this is a reasonable supposition may be seen according to the following argument: the pi-mesons are produced by energetic collisions of the primary cosmic radiation with the nuclei of the air molecules in the upper atmosphere, while the mu-mesons are chiefly products of the heavy meson decay; hence, to reach sea level the pi-meson would have a greater thickness of atmosphere to traverse. Moreover the lifetime of the mu-meson is about 100 times greater than that of the pi-meson while its cross-section for nuclear interaction is roughly one one-thousandth that of the pi-meson (83). Therefore it would be expected that effectively all the pi-component has been removed from the meson beam by the time it reaches sea level. It is fairly reasonable, in view of the above considerations, to identify the penetrating particles as mu-mesons.

(b) Secondaries

The question which now presents itself is what possible interactions could be initiated by the mesons in the aluminum that could give rise to secondaries. The first might be the production of knock-on electrons. As the meson passes through the material the atoms of the material react with the variable electromagnetic field set up by the passing particle. The result is an excitation of the atom and if sufficient energy is transferred, an ionization. The ejected electrons in the ionization process will mostly be of low energy and unable to escape from the material in which they are produced. However, if the distance of closest approach of the meson to the atom is of the order of the atomic dimensions, the interaction is no longer with the atom as a whole but with one of the atomic electrons. As a consequence of the collision, the electron is ejected from the atom with considerable energy and hence will be able to escape from the material and be detected. This phenomenon is described as a knock-on process.

The second interaction might be the production of bremsstrahlung. If the meson passes the atom within the atomic radius, close to the nucleus, the electric field of the nucleus may be sufficient to deflect the fast particle. Such a deflection implies that the fast particle has been accelerated in a direction more or less perpendicular to

its path. This acceleration results in the production of a number of low energy quanta, whose total energy is usually a very small fraction of the particle energy. In some cases, however, one photon of energy comparable with that of the meson is emitted. Such radiation is termed bremsstrahlung. If the photon is of appreciable energy, then there is a finite probability that, through an interaction of the photon with the Coulomb field of a nucleus, the photon will materialize as an electron-positron pair. The electron or perhaps the positron could then escape and be detected by the apparatus.

The third interaction might be direct pair production by the meson. The electromagnetic field of the meson can be considered to be equivalent to a flux of photons. When the particle passes in the neighbourhood of an atomic nucleus, each of its associated "virtual" photons has a certain probability of undergoing a materialization process as for a "real" photon. As in the case above, either the electron or positron or both could activate the apparatus. The proportions of the soft component resulting from these three electromagnetic interactions accompanying the mu-meson at various depths underground have been calculated by S. Hayakawa and S. Tomonaga (84). These calculations give essentially the relative contributions of the three interactions to the secondary radiation accompanying a fast meson as a function

of the thickness of the material through which it has passed. Although their calculations were for underground measurements and the imposed minimum energy of their secondaries was somewhat higher than can be detected by this equipment, their results are applicable to indicate an order of magnitude of importance of the three processes. They find that even at a thickness of about 10^4 gm.-cm.$^{-2}$ the contribution due to pair production is only about 5% of that due to knock-on electrons and the contribution due to bremsstrahlung is even less. Also the knock-on process becomes relatively much more important at smaller thicknesses. Thus it is reasonable to assume that the only electromagnetic interaction of any importance in the production of secondaries in the thicknesses of material used in this experiment is the knock-on process.

Besides the electromagnetic interactions detectable secondaries could be produced through nuclear disintegrations and production of penetrating showers by the mu-meson. As noted previously the cross-section for this process is quite small, being of the order of 10^{-29} cm.^{2} per nucleon. This cross-section corresponds to a collision length, or mean free path, in aluminum of roughly $2 \cdot 10^5$ gm.-cm^{-2}. This is several orders of magnitude greater than any thickness of material used in the experiment, hence, this effect is negligible.

A complimentary verification of the conclusion

that the process producing the secondary particles is the knock-on interaction can be obtained from the experimental results with the absorbers of different atomic numbers. The absorber thickness in gm.-cm.$^{-2}$ in each case is roughly the same. Then, neglecting the complications of absorption in the materials, the expected variation of the number of secondaries produced as a function of the material can be estimated qualitatively as follows. If the processes are knock-on electrons then the number produced should vary as the number of electrons present in the material, i.e., as Z/A where Z is the atomic number and A the mass number. Hence, there should be about 25% more secondaries produced in the carbon than what would be produced in the lead. On the other hand if the method of production is by bremsstrahlung or pair production the variation of numbers detected would be proportional to Z^2/A, or the number emerging from the lead could be roughly 10 times greater than that emerging from the carbon. Finally, if the secondaries are the results of nuclear interactions then their number would be constant for equal gm.-cm.$^{-2}$ thicknesses of materials.

The actual ratio of the number of secondaries produced per 1000 mesons in carbon to that in lead is 1.4 ± 0.2, in good agreement with that to be expected from the knock-on process. The experimental data are quite inconsistent with the assumption that the

bremsstrahlung or pair-production mechanisms are important.

3.6 Theoretical Calculations

Since it is reasonably certain that the phenomenon represented by the observations taken with the present apparatus represents the production of knock-on electrons by cosmic ray mesons, it is worthwhile to consider this process in some detail. In particular it would be desirable to compare the experimental results with those expected from theoretical considerations. Therefore, in what follows, an attempt is made to calculate the probability that a cosmic ray meson, in passing through an aluminum plate, will produce a knock-on electron which could be detected by the apparatus, as a function of the thickness of the plate. The method used in the calculation is similar to that given by F. L. Hereford (85).

(a) Calculation of Knock-on Frequency

In order to simplify the algebraic form of the equations of this section, it will be convenient to give the energies of the mesons and electrons in units of their respective rest energies and the momenta of the particles in units of their rest energies divided by c, the velocity of light.

Consider the collision of a meson of spin $\frac{1}{2}$, charge e, rest mass M and momentum p with an electron of rest mass m, which is ejected at an angle θ

with respect to the incident meson direction and with energy between E and $E + dE$.

Then the conservation laws yield the following expression for the electron energy.

$$E = \frac{2p^2 \cos^2 \vartheta}{[(m/M) + (p^2 + 1)^{\frac{1}{2}}]^2 - p^2 \cos^2 \vartheta} \qquad [1]$$

The maximum transferable energy corresponds to a "head-on" collision, i.e., $\cos \theta = 1$, therefore

$$E_m = \frac{2p^2}{(m/M)^2 + 1 + (2m/M)\ (p^2 + 1)^{\frac{1}{2}}} \qquad [2]$$

since $M \simeq 200\ m$ then $(m/M)^2$ can be neglected and setting $1 + 0.01\ (p^2 + 1)^{\frac{1}{2}} = k$, [2] becomes $E_m = 2p^2/k$

Also rearranging [1] yields

$$\cos \theta = \left[\frac{p^2 + k}{p^2}\right]^{\frac{1}{2}} \left[\frac{E}{E + 2}\right]^{\frac{1}{2}} \qquad [3]$$

The probability that such a collision will occur when the meson traverses a thickness dx (gm.-cm.$^{-2}$) of material as calculated by Bhabha (86) and by Massey and Corben (87) is

$$P(p,E)\ dE = 2C\ \left(\frac{1 + p^2}{p^2}\right) \frac{dE}{E^2} \left[1 - \frac{k}{2(1 + p^2)} E + \frac{1.25 \cdot 10^{-3}}{1 + p^2} E^2\right] \qquad [4]$$

where $C = \pi N r_e^2 Z/A = 0.15\ Z/A$ gm.$^{-1}$cm.^{2}. Z and A are the charge and mass number of the material, N is Avogadro's

number, and $r_e = e^2/mc^2$ is the classical radius of the electron. Thus C represents the total "area" covered by the electrons contained in 1 gram, each considered as a sphere of radius r_e.

In order for the knock-on electron to be counted, it must have sufficient energy to penetrate the counter wall and enter the sensitive volume. The thickness of the glass and carbon forming the counter wall (0.24 ± 0.01 gm.-cm.$^{-2}$) corresponds to the range of an electron with energy $1.3\ mc^2$. Thus the minimum energy that the electron must have, upon emerging from the aluminum, is $1.3\ mc^2$ in order to be detected.

If the knock-on is produced in the interval between x and $x + dx$ (Figure 5) there exists an energy E_o such that the energy on emergence from the material is $1.3\ mc^2$. Thus, if $Q(E,x)$ is the probability that an electron of energy E produced in the interval between x and $x + dx$ is counted,

$$Q(E,x) = \begin{cases} 1 & \text{for } E \geq E_o \\ 0 & \text{for } E < E_o \end{cases}$$

It, therefore, follows that the frequency of production of a detectable knock-on electron by a meson of momentum p in a thickness x_o gm.cm.$^{-2}$ of material is given by

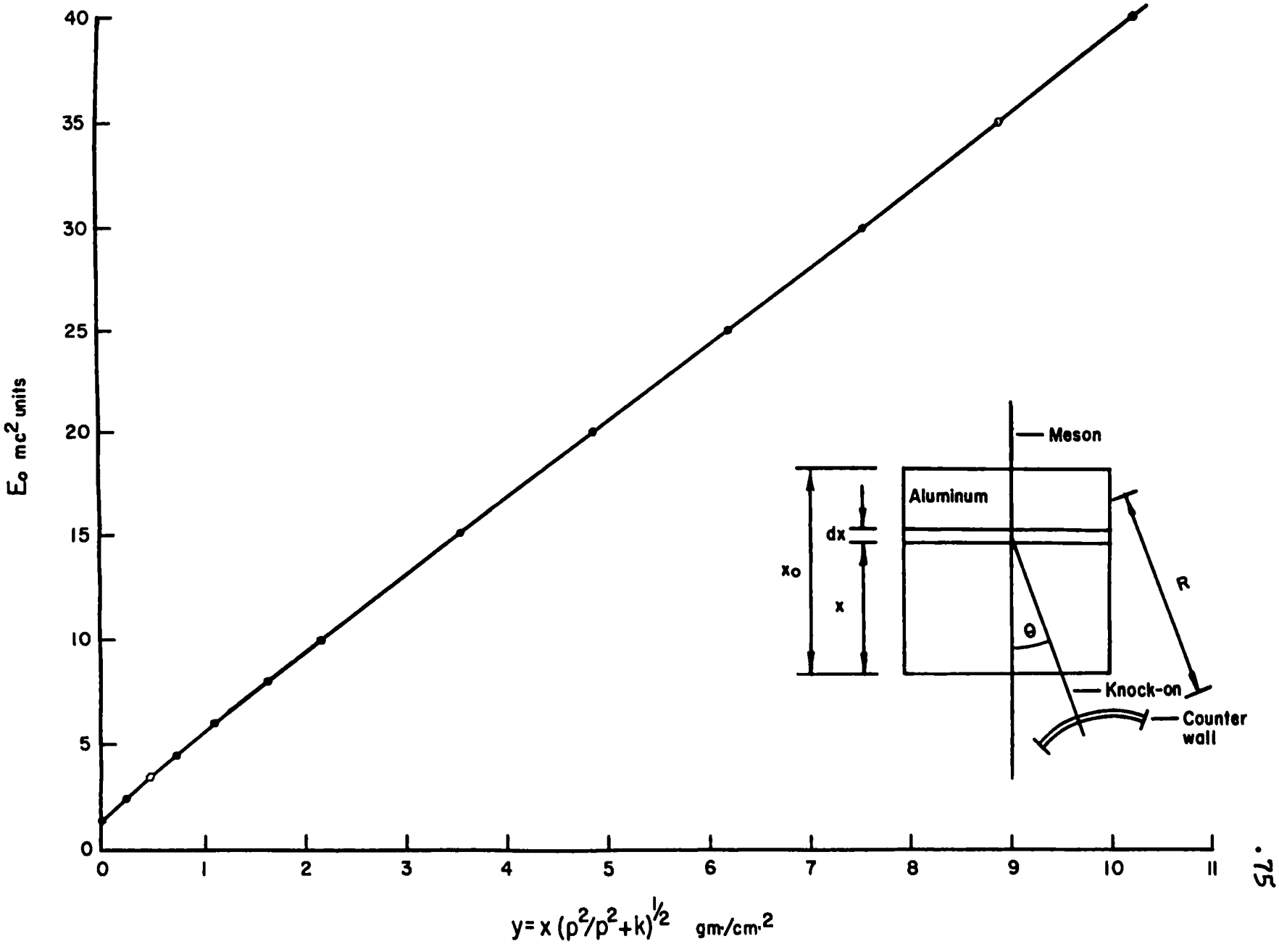

FIG. 5. Variation of minimum knock-on energy E_o with production layer height

$$f(p,x_o) = \int_0^{x_o} \int_{E_o(x)}^{E_m(p)} P(p,E)\, dE\, dx \qquad [5]$$

The function $E_o(x)$ can be obtained from the following considerations. In order to be counted, the range $R(E)$ of the electron must be greater than $(x/\cos\theta) + 0.24$. Therefore, $R(E_o) = (x/\cos\theta) + 0.24$ or using equation [3]

$$\left[\frac{p^2}{p^2 + k}\right]^{\frac{1}{2}} x = \left[R(E_o) - 0.24\right] \left[\frac{E_o}{E_o + 2}\right]^{\frac{1}{2}} \qquad [6]$$

The expression for the electron range given by Katz and Penfold (74) when transferred to the units used in this work appear as

$$R = 0.195\, E^{1.20} - 0.095\, \ln E \qquad \text{for } 0.2 < E \leq 5$$

$$R = 0.270\, E - 0.106 \qquad \text{for } 5 < E \leq 40$$

Using these relationships, numerical values of the right-hand side of equation [6] can be calculated for various values of E. These values are plotted as descrete points on the graph of Figure 5 with E_o as the ordinate. The curve shown on the graph is represented by tho functions

$$\frac{3.72y + 1.94}{1 + 0.492 \exp.\ (-3.9y^{0.76})} \qquad \text{for } x \leq 1$$

and

$$3.72y + 1.94 \qquad \text{for } x > 1$$

where $$y = \left[\frac{p^2}{p^2 + k}\right]^{\frac{1}{2}} x$$

Thus we can represent E_o as a function of x and p to a close approximation by the expression

$$E_o(x) = (Ax + B)/(1 + 0.492z) \qquad \text{for } x \leq 1$$

and [7]

$$E_o(x) = Ax + B \qquad \text{for } x > 1$$

where $A = 3.72\ p/(p^2 + k)^{\frac{1}{2}}$, $B = 1.94$, and $z = \exp.\ (-3.9x^{0.76})$.

Carrying out the integration of equation [5] with respect to the electron energy to obtain the function

$$F(p,x) = \int_{E_o(x)}^{2p^2/k} P(p,E)\ dE$$

yields

$$F(p,x) = 2C\left[\frac{1 + p^2}{p^2}(1/E_o) + \frac{k}{2p^2}\ln E_o - \frac{1.25 \cdot 10^{-3}}{p^2} E_o + K\right] \qquad [8]$$

where $K = \frac{2.5 \cdot 10^{-3}}{k} - \frac{k(1 + p^2)}{2p^4} - \frac{k}{2p^2} - \frac{k}{2p^2}\ln(2p^2/k)$ is

independent of x.

Substituting the appropriate expression for E_o gives

$$F(p,x) = \begin{cases} N(p,x) + M(p,x) & \text{for } x \leq 1 \\ N(p,x) & \text{for } x > 1 \end{cases}$$

where

$$N(p,x) = 2C \left[\frac{1 + p^2}{p^2} \frac{1}{Ax + B} + \frac{k}{2p^2} \ln(Ax + B) - \frac{1.25 \cdot 10^{-3}}{p^2} (Ax + B) + K \right]$$

and

$$M(p,x) = 2C \left[\frac{0.492z}{Ax + B} + \frac{1.25 \cdot 10^{-3} z\,(Ax + B)}{p^2(1 + 0.492z)} - \frac{k}{2p^2} \ln(1 + 0.942z) \right]$$

Therefore, it follows:

$$f(x_o,p) = \int_o^{x_o} N(p,x)\,dx + \int_o^{x_o} M(p,x)\,dx \quad \text{for } x_o \leq 1$$

and [9]

$$f(x_o,p) = \int_o^{x_o} N(p,x)\,dx + \int_o^{1} M(p,x)\,dx \quad \text{for } x_o > 1$$

The first integral can be treated analytically and gives the result

$$I(p,x_o) = \int_o^{x_o} N(p,x)\,dx$$

$$= 2C\left\{\ln(Dx_o + 1)\left[\frac{1 + p^2}{Ap^2} + \frac{k(Dx_o + 1)}{2Dp^2}\right]\right.$$

$$- x_o\left[\frac{k}{2p^4} + \frac{k}{p^2} + \frac{1.25 \cdot 10^{-3}}{p^2}B - \frac{k}{2p^2}\ln\frac{Bk}{2p^2} - \frac{2.5 \cdot 10^{-3}}{k}\right]$$

$$\left. - x_o^2\left[\frac{1.25 \cdot 10^{-3}}{2p^2}A\right]\right\} \qquad [10]$$

where $k = 1 + 0.01\,(p^2 + 1)^{\frac{1}{2}}$, $A = 3.72\,p/(p^2 + k)^{\frac{1}{2}}$, $B = 1.94$, and $D = 1.92\,p/(p^2 + k)^{\frac{1}{2}}$. The second integral of equation [9] is not readily integrated analytically but since for values of $x > 1$ it is a constant, only a few numerical integrations are needed.

Thus far the calculations have yielded the frequency, $f(p,x_o)$, of emergence of a detectable knock-on electron as a function of the production material thickness x_o, for a meson of a given momentum, p. The next step is to integrate the frequency over the momentum spectrum of the cosmic ray mesons at sea level. This is most readily done numerically. To facilitate this procedure, the variation of $f(p,x_o)$ as a function of p is determined for various fixed values of x_o. Those curves are shown in Figure 6. Also shown is the sea level meson momentum spectrum for p less than 100 Mc. It is

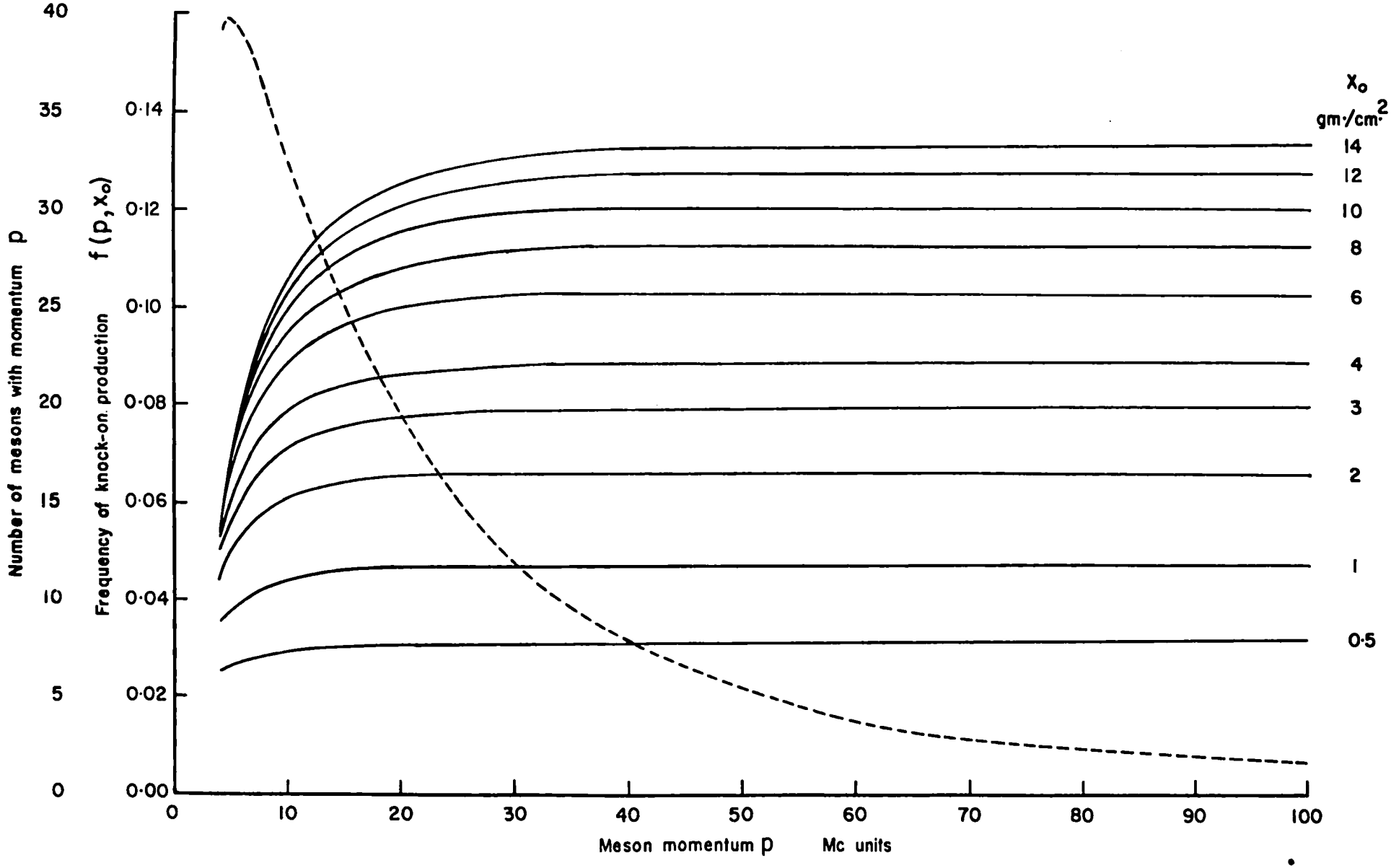

·80·

FIG·6· Frequency of knock-on production as a function of Aluminum thickness x_o and incident meson momentum p (solid curves)· Sea-level meson momentum spectrum (dashed curve)·

essentially that as given by Rossi (88). The minimum momentum acceptable by the telescope is determined by the 20 cm. of lead above counter 3. In order to be able to traverse this much lead the meson must have a momentum greater than 4 Mc. The momentum spectrum is normalized so that there are 1000 mesons with momenta greater than this lower limit, assuming that the spectrum decreases as $1/p^3$ for $p > 100$ Mc (89). The mesons are treated as consisting of two momentum groups. Since the values of $f(p,x_o)$ are essentially constant with respect to p for values of $p > 100$ Mc, the number of knock-ons produced by the mesons in the first momentum group, for a given thickness of material, is simply obtained by multipling the constant value of $f(p,x_o)$ by the total number of mesons with momenta greater than 100 Mc. The second group consists of the mesons whose momenta lie between 4 and 100 Mc. For this group the number of knock-ons emerging from a given thickness is obtained by multipling the function $f(x_o,p)$ for the particular thickness, by the momentum spectrum and integrating numerically. The final curve is then obtained by adding together the contribution of each group for the different thicknesses. The resultant curve is shown in Figure 7.

Also shown in Figure 7 are the curves that correspond to knock-on electrons which could traverse the thickness of material between the various trays. The

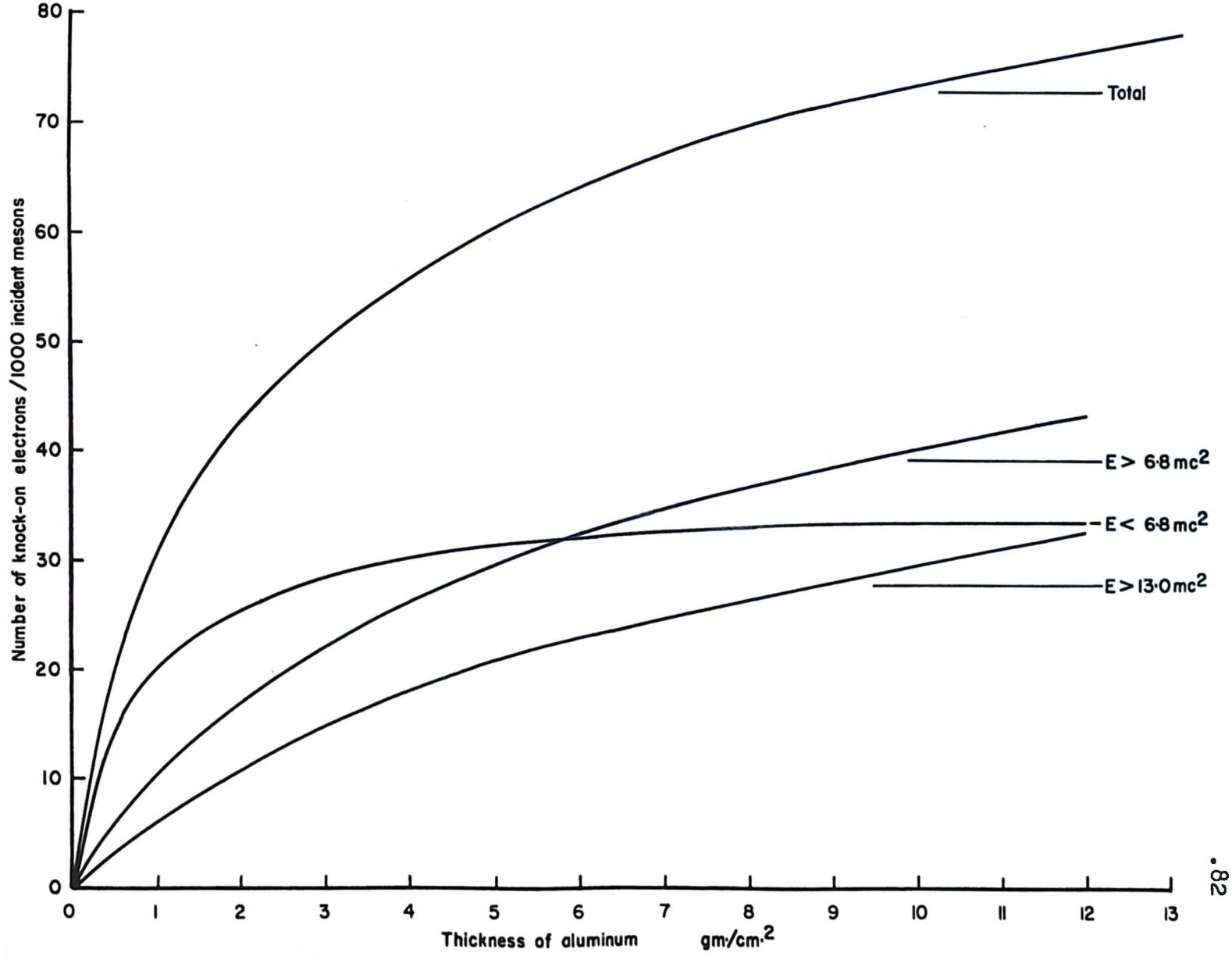

FIG. 7. Number of knock-ons versus thickness of production material for various electron emergent energies E.

thickness of material between trays a and b is 1.31 gm.-cm.$^{-2}$. In order for an electron to be able to traverse this thickness and still have sufficient energy to trigger tray b, its initial energy must be in excess of 6.8 mc^2. For the electron to reach tray c and be counted by it, its initial energy on emerging from the aluminum above tray a must be in excess of 13.0 mc^2.

(b) Comparison of Calculated and Experimental Results

One important factor which has not been considered is the efficiency of the telescope to detect the emerging knock-on electrons. In order to compare the calculated and experimental results, the latter require correction for this efficiency. However, an estimate of this efficiency will be reserved till later. Instead, it will be assumed that the only factor which is important is a geometric one, and that the angular distribution of the knock-ons emerging from different thicknesses is the same. Therefore, if the experimental results are in agreement with the calculated values, then the following equation should hold for all thicknesses of the material.

$$N_e = \epsilon N_c + N_o$$

Where N_e is the number of knock-ons per 1000 mesons as detected by the apparatus, N_c is the calculated number of knock-ons per 1000 mesons that should be detected. N_o is the number of background counts, and ϵ is the

efficiency of detection of the knock-ons by the apparatus, ϵ and N_o being constant.

By comparing the values of N_e and N_c for the same thickness of material for the various events observed, the best values for ϵ and N_o can be determined by the method of least squares. The results are given in Table IX.

TABLE IX

The experimental and calculated number of events per 1000 mesons, and the values for efficiency and background as determined by the method of least squares.

a		A		AB + ABC		ABC	
Exp.	Calc.	Exp.	Calc.	Exp.	Calc.	Exp.	Calc.
19.0	0	8.5	0	9.0	0	8	0
37.5	20.5	18.5	14.5	19	7	10	3.2
49.5	35.5	27.5	22.7	22.5	12.7	12.5	7.7
53	44.6	27	26.5	26.5	18.2	17.5	11.7
64	50.6	32	28.5	31	22.3	20	15.0
65	55.1	33.5	29.9	32	25.8	22	17.6
69	59.0	33	30.9	35.5	28.7	21	19.9
74	62.2	33.5	31.7	39.5	30.9	26.5	21.7
75.5	65.1	34.5	32.2	38	33.1	27	23.4
78.5	67.5	32.5	32.6	46.5	34.9	31	24.9
72	69.5	34	32.8	38	36.5	27	26.3
76	71.3	37.5	33.0	38.5	38.0	27	27.8
76	74.1	37	33.5	40.5	40.8	29	30.4
83	78.1	34	33.9	49	44.6	35	34.2
$N_o = 20.4$		$N_o = 7.9$		$N_o = 12.0$		$N_o = 7.9$	
$\epsilon = 0.804$		$\epsilon = 0.817$		$\epsilon = 0.798$		$\epsilon = 0.769$	

The calculated results that are used to represent the A, AB + ABC, and ABC events are obtained from the theoretical curves for different emergent energies of the

knock-on electrons. The A events are associated with the curve, that represents the knock-ons emerging with energies less than 6.8 mc^2, i.e., those that are unable to penetrate the material between trays a and b. The AB + ABC events are associated with the curve, which represents the number of knock-ons that can fire the b tray, i.e., those which have energies in excess of 6.8 mc^2. The ABC events are associated with the curve for knock-ons which emerge with energies greater than 13.0 mc^2 and hence, are able to fire all three trays.

The experimentally determined number of secondary electrons and the calculated curves corrected for efficiency and background using data from Table IX are shown in Figures 8 and 9.

If the assumption that the efficiency and background are constant is valid then the results indicate, that within experimental error, there is no discrepancy in the variation of the number of knock-ons per 1000 mesons emerging from an aluminum plate, with the thickness of the plate, as determined experimentally and calculated theoretically. Furthermore the agreement holds for knock-ons of the different energy ranges that are distinguishable in this experiment. However, at this point, nothing can be said about any agreement of the absolute numbers of knock-ons emerging from the plate since the actual efficiency of detection is not known.

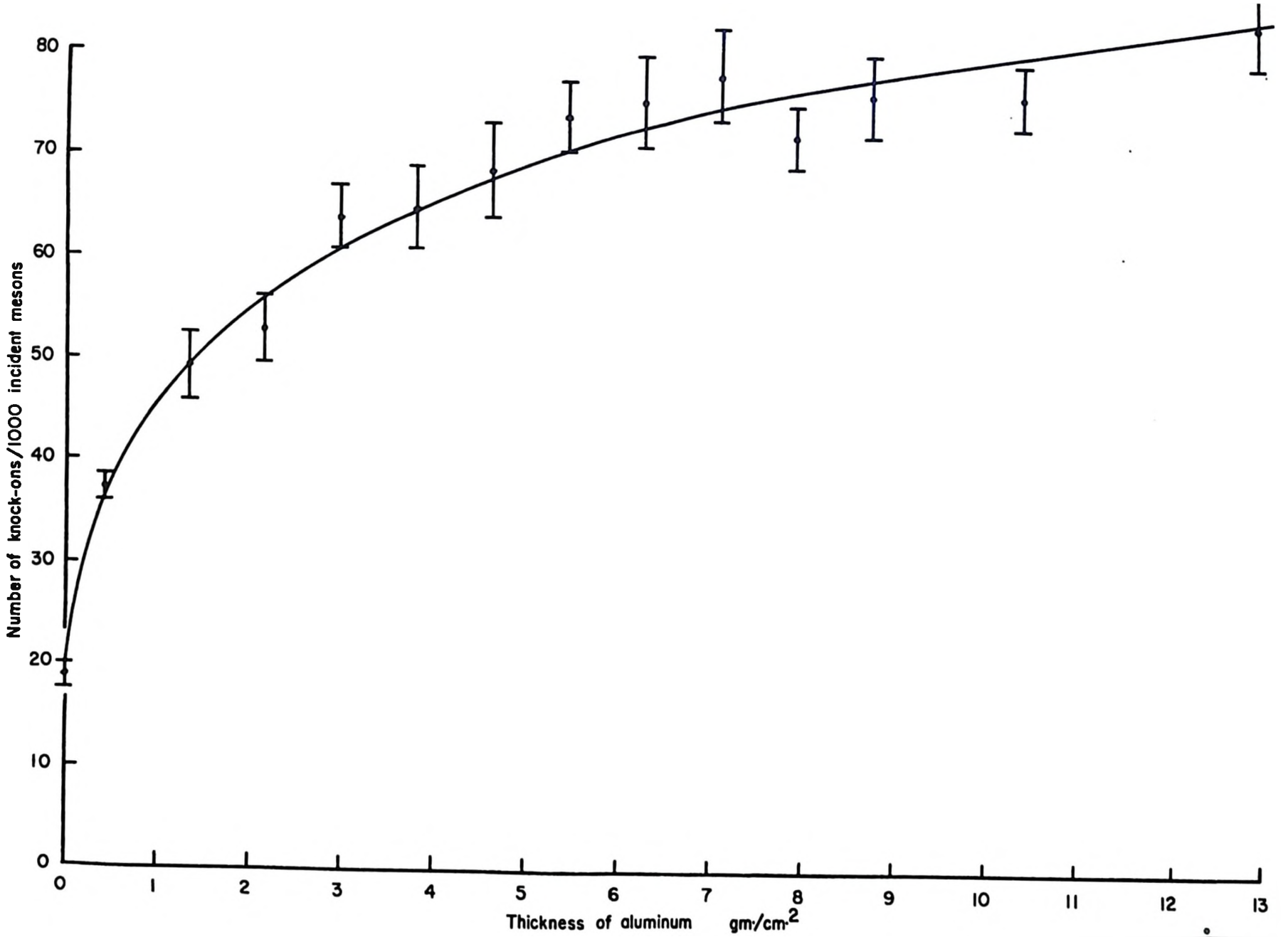

FIG. 8. Number of detectable knock-ons versus thickness of production material, showing the experimental points & calculated curve adjusted for efficiency & background.

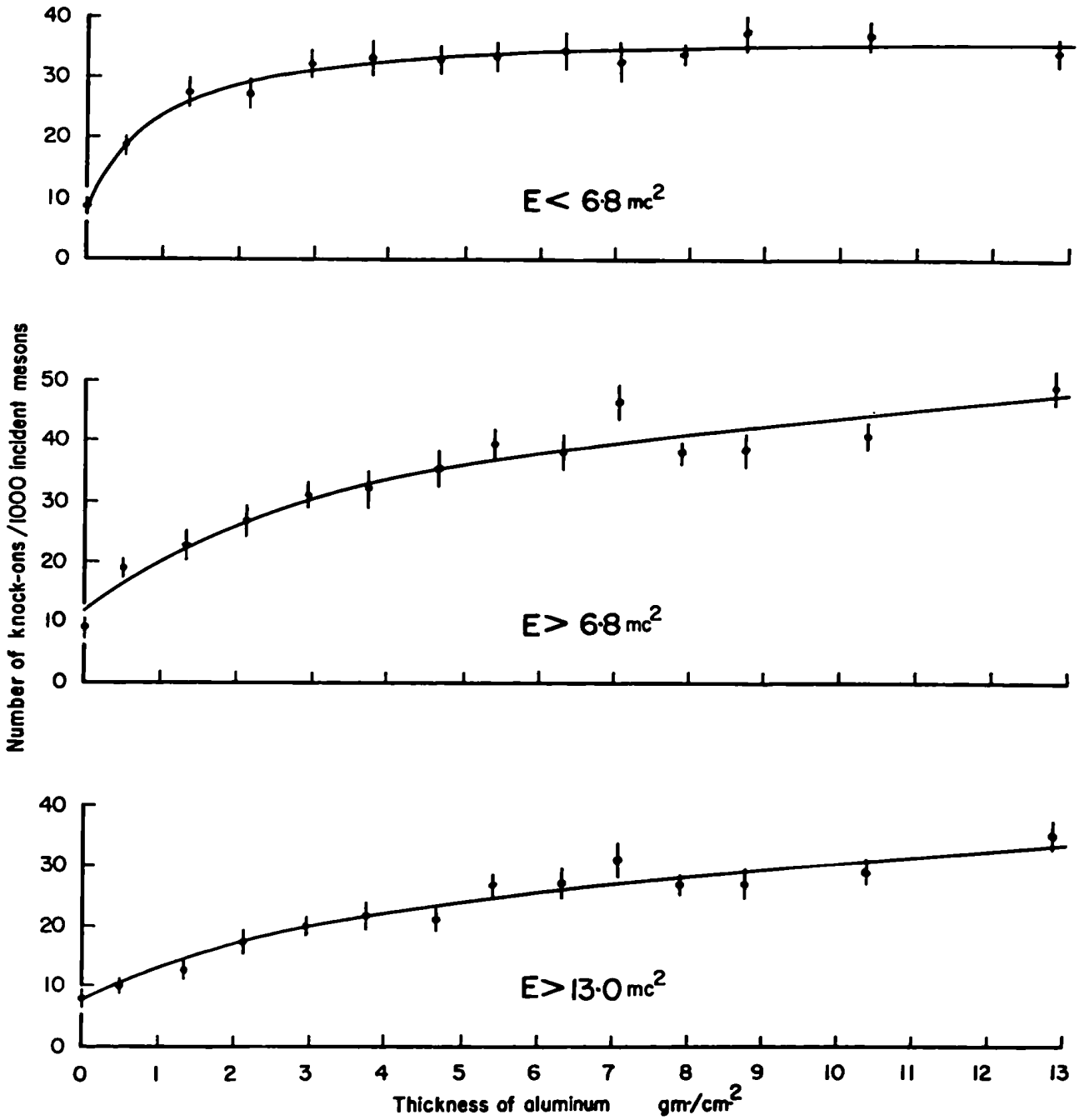

FIG. 9. Number of detectable knock-ons versus thickness of production material, showing experimental points & calculated curves adjusted for efficiency & background; for various emergent energies E.

It is also of some interest to note the variation of the number of knock-ons with equal thicknesses of different materials. It has already been set forth that observations were taken with approximately equal thicknesses of carbon, iron and lead in addition to the aluminum. The results are given in Table VIII. Also since the number of secondary electrons varies as the Z/A of the material in which these are produced, the results have been plotted against the Z/A for the substances used and shown in Figure 10. Also shown is the expected variation (dashed curve) assuming that the absorption within the producing medium is the same in all cases as for aluminum. The experimental results are linear within experimental error, but indicate a decrease from the expected number for a heavier material. If this effect is real, it could be reasonably attributed to an increase in absorption within the material or perhaps a difference in efficiency of detection due to a dependence of the angular distribution of the knock-ons on the material in which they are produced. Some doubt, perhaps, is thrown on the validity of these results when the relative numbers of knock-ons of various energies are considered for the different materials. Expressing these as percentages of the total number, the results are:

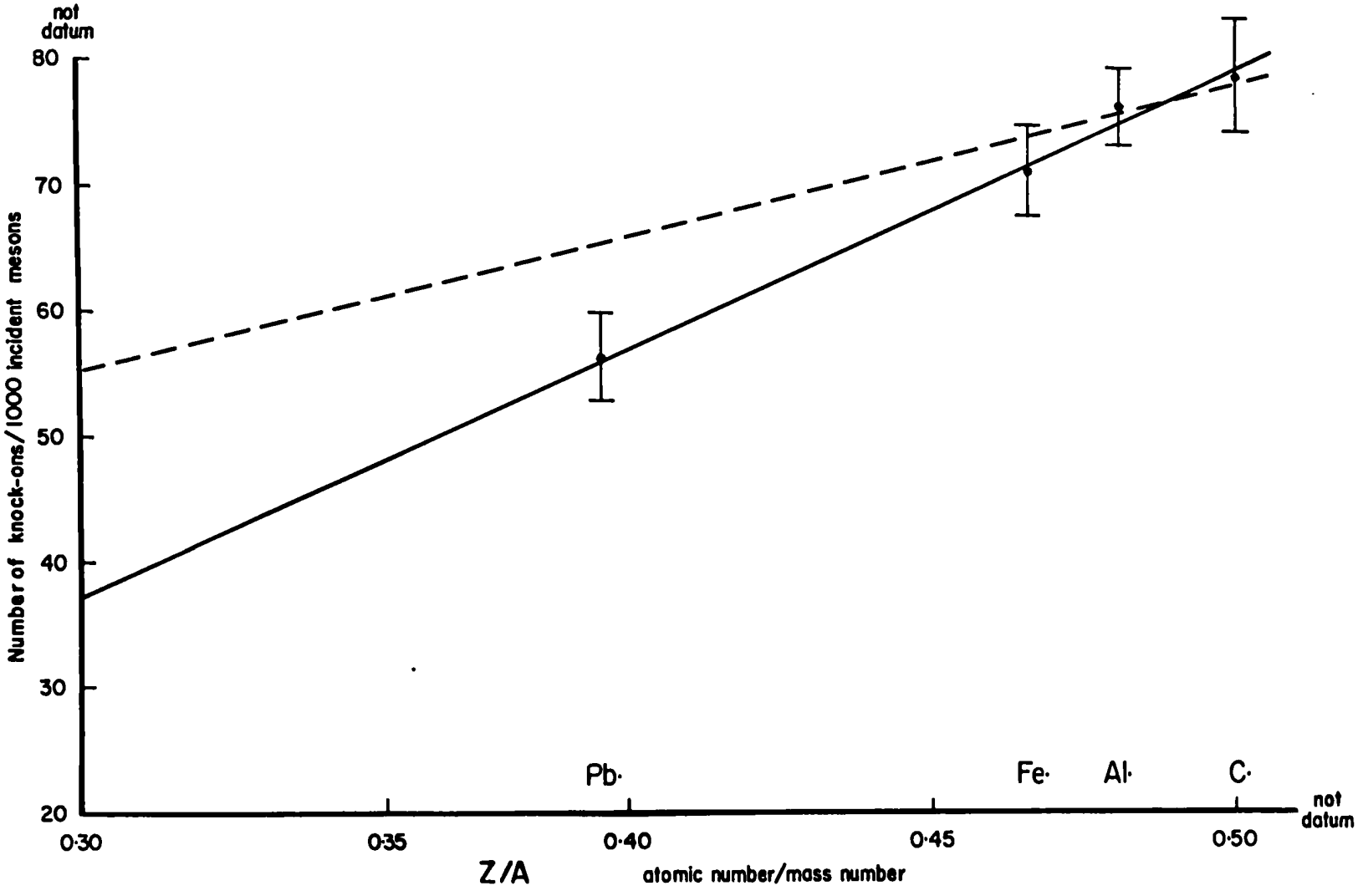

FIG· 10· Number of detectable knock-ons from equal gm·/cm·^{2} of various materials as a function of Z/A of the material· Dashed line assumes equal absorption, solid is best fit·

Material/Energy of Knock-on	$<6.8\ mc^2$	$>6.8\ mc^2$	$>13.0\ mc^2$
Carbon	50 ± 5%	50 ± 5%	40 ± 4%
Aluminum	49 ± 3%	51 ± 3%	37 ± 3%
Iron	53 ± 5%	47 ± 5%	32 ± 4%
Lead	39 ± 5%	61 ± 6%	46 ± 5%

The accuracy of the measurements does not allow definite conclusions, but the indications are that there is a decrease in the number of low energy electrons emerging from the lead with respect to the number that emerges from the carbon, while the number of high energy electrons does not appreciably change for the different materials. This is opposite to what would be expected. The energy loss per gm.-cm.$^{-2}$ of low energy electrons (i.e., those which lose energy chiefly by ionization) is loss in lead than in carbon. Hence the numerous knock-ons of low energy produced in the last few gm.-cm.$^{-2}$ of the material should escape more readily from the lead than from the carbon. On the other hand, the energy loss of high energy electrons (when bremsstrahlung becomes important) is much greater in the lead. Thus there should be a degradation of the relative number of high energy knock-ons emerging from the lead over that emerging from the carbon. The energy loss per gm.-cm.$^{-2}$ in the two materials is equal for electrons of approximately 8 mc^2 energy.

The differences due to the variation in energy loss may be offset somewhat by a change in efficiency of detection. High energy electrons emerge at small angles

to the meson direction and many miss being counted because they pass through the same counter as the meson. However, there is a possibility that the electron will be scattered or will initiate a shower in the material, thereby increasing its chance of firing the tray. Since the probability of doing this is greater for the secondaries produced in the lead, there is a greater efficiency for detecting high energy knock-ons produced in the lead. In addition, since there is a possibility of a larger scattering of the low energy secondaries in the lead than in the carbon, more low energy electrons will be scattered out of the telescope in the case of the lead and thereby lost.

Thus these differences produce effects that are opposite to those caused by the differences in energy loss. As to what resultant effect would be expected, depends upon which is the chief cause and this is not readily determined.

(c) Calculation of Knock-on Detection Efficiency

In order to determine if the observed frequency of production of knock-ons is in agreement with the calculated frequency, an attempt is made, in what follows, to estimate the efficiency of detection of the knock-ons. The discussion will be limited to the a events so as to confine the calculations to the efficiency of tray a only.

The basic requirement for a consideration of the

geometric efficiency is a knowledge of the angular distribution of the knock-ons about the incident meson direction. Brown, et al. (67), have studied the angular distribution of knock-on secondaries of penetrating particles using both cloud chamber and Geiger counters. These authors found that the probability $P(\theta)$ that the knock-on will emerge from the material into a solid angle $d\omega$, making an angle θ with its primary is given by

$$P(\theta)\, d\omega = k \cos^{2.5}\theta \, d\omega \qquad [11]$$

The above form of the empirical expression was obtained from the cloud chamber observations. However, the results yielded by their coincidence counter method were found to be in agreement with this expression within experimental error ($\sim$ 20%). Furthermore their counter experiments indicate that the distribution is relatively independent of the nature and thickness of the knock-on producing material. Hence, the restriction to be used in the following calculations, that the angular distribution is independent of thickness of material has some basis of experimental justification. A further approximation will be made in that the angle will be measured not from the point of production but from the point of emergence from the material.

The tray configuration chosen for the present experiment does not readily lend itself to a straight-

forward calculation of the geometrical efficiency of detection. However, an estimate can be made by considering the counters to be infinitely long, thereby simplifying the calculations by requiring a consideration of the angular distribution and efficiency in the lateral plane only. This lateral efficiency can then be corrected for end effects due to the finite length of the counters.

Consider the typical knock-on event illustrated in Figure 11(a) (not to scale). The meson enters the telescope vertically at a lateral distance x and longitudinal distance y from the vertical axis of the instrument, knocking-on a secondary in passing through the aluminum (not shown). The secondary emerges at an angle θ with respect to the primary direction and fires one of the upper outside counters of the tray and is thereby detected.

The projected angle in the lateral plane is designated by β and the projected path length between emergence from the material and entrance into the counter is designated by D. (The lateral projection is also shown separately in (b) part of the same Figure.) The angle α is the angle between the actual trajectory of the secondary electron and its lateral projection.

Making use of the angular distribution of the probability of knock-on production, as given by equation [11], in conjunction with the relations,

and

$$\cos\theta = \cos\alpha \cos\beta$$

$$d\omega = \cos\alpha \, d\alpha \, d\beta$$

one obtains, for the probability $p(\beta)$ that the electron will emerge from the material in the projected angular interval β to $\beta + d\beta$, the expression

$$p(\beta)\, d\beta = K \cos^{2.5}\beta \, d\beta \qquad [12]$$

where

$$K = k \int_{-\pi/2}^{\pi/2} \cos^{3.5}\alpha \, d\alpha \qquad [13]$$

Thus, under the assumption that the telescope is of infinite length, the lateral efficiency is given by the fraction

$$\int_{-\beta_L}^{\beta_U} p(\beta)\, d\beta \Big/ \int_{-\pi/2}^{\pi/2} p(\beta)\, d\beta$$

where the limits $-\beta_L$, β_U are determined by the geometry of the detecting tray. The actual values of these angular limits depend upon the lateral distance at which the meson enters the telescope. Therefore, the efficiencies for various lateral displacements need to be determined and averaged in order to ascertain the mean lateral efficiency.

This is accomplished in the following manner.

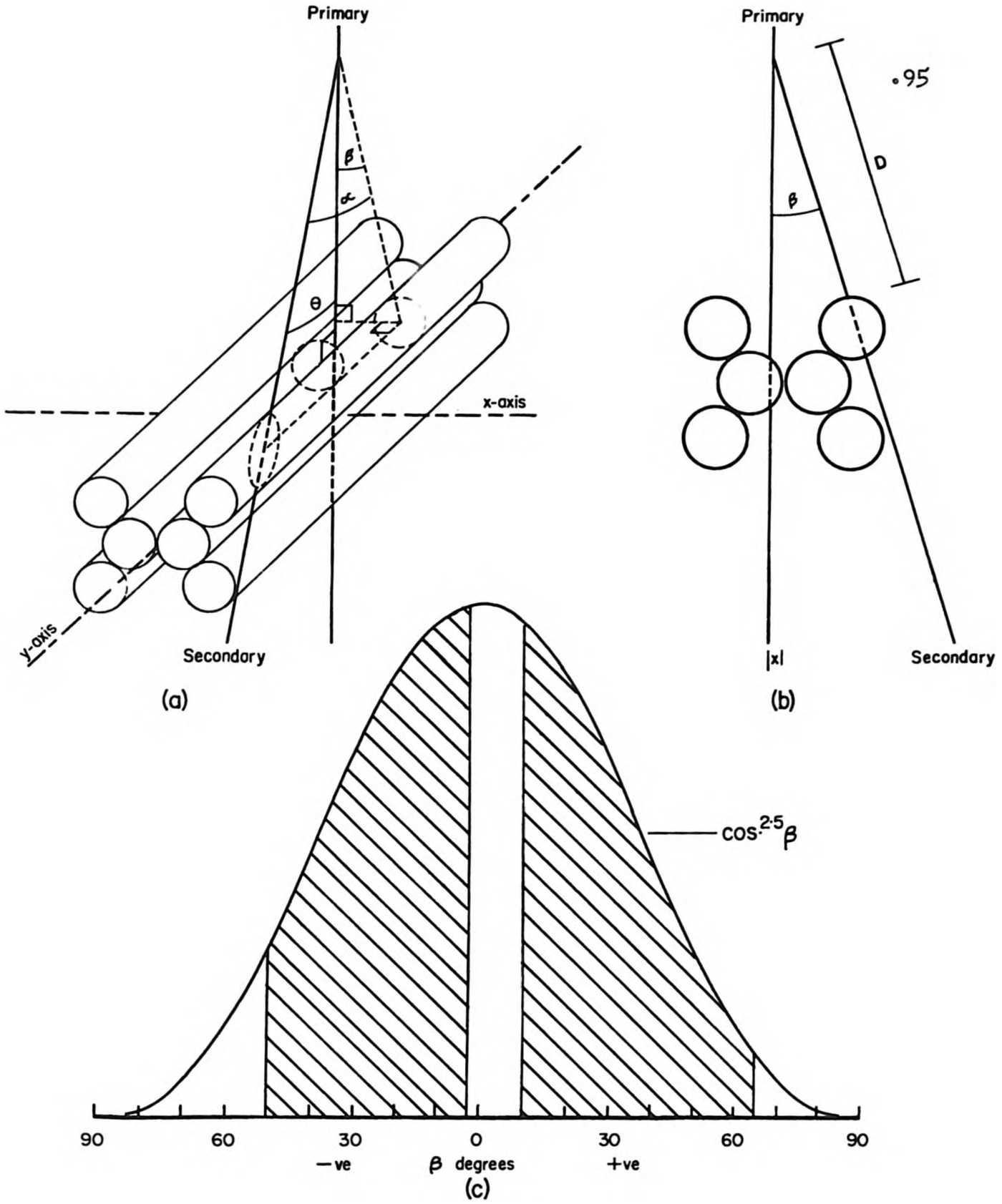

FIG. 11 Illustrative knock-on event for efficiency calculations,
(a) the defining angles (b) lateral projection (c) angular distribution

Consider further an event of the type illustrated in Figure 11(b) along with the curve of $\cos^{2.5}\beta$ shown in part (c). For the lateral displacement x = - 0.5 inches, if the angle β is greater than -3 degrees but less than + 10 degrees the secondary passes through the same counter as the meson and hence is not detected. If, however, the electron trajectory lies within either of the angular intervals + 10 to + 65 degrees or -3 to -50 degrees then it passes through a sensitive counter and the particle is detected. Should the path lie outside these two angular intervals the secondary would miss the tray completely. It, therefore, follows that the efficiency of detection for this displacement is given by

$$\int_{-50^\circ}^{-3^\circ} p(\beta)\, d\beta + \int_{10^\circ}^{65^\circ} p(\beta)\, d\beta \Bigg/ \int_{-90^\circ}^{90^\circ} p(\beta)\, d\beta$$

or it is represented by the ratio of the hatched area in Figure 11(c) to the total area under the curve. This ratio is readily determined by means of a planimeter.

In this way the efficiency for various selections of x-displacement values are determined. The results are set forth in Table X.

TABLE X

Values of the efficiency of detection for various lateral displacements.

Lateral Displacement x in inches	Efficiency of Detection in per cent
0	85.6
0.1	83.9
0.2	83.2
0.3	81.6
0.4	80.9
0.5	79.9
0.6	78.3
0.7	77.1
0.75	76.7
Mean	81.1

Thus, the mean lateral efficiency as determined by this method is 81.1%.

In considering the possible effect of the finite length of the counters, it is seen that it influences the efficiency by altering the limits of integration in the expression for K as given by equation [13]. In the example illustrated, for instance, the limits of variation of α are not $-\pi/2$ to $\pi/2$ but rather arc tan $D/(y - L)$ and arc tan $D/(y + L)$ where $2L$ is the length of the counter and equals 20 inches. Thus the fraction of knock-ons emerging at the indicated projected angle that are detected is given by

$$F = \int_{\arctan D/(y-L)}^{\arctan D/(y+L)} \cos^{3.5}\alpha \; d\alpha \Big/ \int_{-\pi/2}^{\pi/2} \cos^{3.5}\alpha \; d\alpha \qquad [14]$$

It is obvious that this ratio is not constant but depends upon y and D which in turn depends upon β. However, if a mean value $\bar{F}$ is determined then an average overall efficiency of detection is given by $\bar{F}$ times the lateral efficiency. In order to estimate $\bar{F}$ the first requirement is to obtain a realistic mean value of the distance D for any value of x or β.

For a given value of x an effective value of D can be defined by

$$D_{eff.} = \int D \cos^{2.5}\beta \; d\beta \Big/ \int \cos^{2.5}\beta \; d\beta$$

where the limits imposed on the integration are the limits of detectability (i.e., set by the insensitive counter and geometrical configuration) and the value of D is the geometrical distance from the point of emergence from the material to the counter wall at the given angle β. Using this definition the following values of $D_{eff.}$ are obtained

Lateral Displacement x in inches	$D_{eff.}$ in inches
0	2.43
0.375	2.42
0.75	1.93
	Mean $\overline{D}$ = 2.28

This mean value $\overline{D}$ = 2.28 inches now allows the evaluation of F for various values of y by graphically integrating the expression $\cos^{3.5}\alpha$ within the appropriate limits as given by equation [14]. Upon carrying out this operation the values of F given in Table XI are obtained.

TABLE XI

Values of the longitudinal correction factor for various longitudinal displacements.

Longitudinal Displacement y in inches	Longitudinal Correction Factor F
0	0.500
1	0.801
2	0.937
3	0.981
4	0.994
5	0.997
6	0.999
7	1.000
8	1.000
9	1.000
10	1.000
	Mean 0.958

Having now obtained $\bar{F} = 0.958$ the overall efficiency ϵ of detection of the knock-ons by the a tray can be evaluated by $\epsilon = \bar{F}$ times the lateral efficiency and so $\epsilon = 78\%$.

In order to estimate how realistic this value may be, the various assumptions made in the calculations must be considered. The question of angular distribution has already been discussed and the assumption shown to be reasonable. The calculations have been carried out assuming vertically incident mesons only and this is not exactly true physically. This vertical collimation is effected to a very close approximation in the lateral plane since the maximum angle of inclination, in this plane, of the meson trajectory with the vertical is only 1.6°. In the longitudinal plane, on the other hand, the maximum angle of inclination is 21°, thus collimation is not so effectively achieved. This acceptance of other than vertical mesons by the telescope will influence the value of F by altering the limits of detection. However, the resultant influence should be relatively small since when the upper limit is increased the lower limit is decreased and the effect is more or less self-compensating.

The intrinsic efficiency of the counters themselves for the detection of electrons would influence the overall efficiency of detection. However this effect is negligible because the intrinsic efficiency for charged particles

that enter the sensitive volume of the counters is very close to unity and it is essentially physically impossible for the knock-ons to pass between the counters.

The only appreciable uncertainity involved in the calculation seems to be in the estimating of the value for $\bar{D}$. A reasonable maximum error in this evaluation is believed to be of the order of 25%. Thus since the longitudinal correction is only 4%, the uncertainty expected in the calculated efficiency is approximately 1%. It can, therefore, be stated rather confidently that the efficiency of the a tray to detect the knock-on electrons is $\epsilon = (78 \pm 1)\%$.

3.7 Conclusions

It has been shown in section 3.6 (b) that with the assumption that the efficiency is of a constant geometrical nature and that the background is also constant, there is satisfactory agreement between the calculated and experimental knock-on production curves for aluminum. In addition, in section 3.6 (c) it has been argued that the constant efficiency assumption is justifiable and a calculated value of $(78 \pm 1)\%$ has been determined. This calculated value is in excellent accordance with the value of $(80 \pm 3)\%$ required for agreement between the experimental and calculated curves. Furthermore since the background determined by a least square fit of the complete curve

agrees very well with that measured at zero thickness, it seems legitimate to assume the background to be constant. By reason of the agreements stated above it can be concluded fairly certainly that the calculated curve represents the actual variation of the number of knock-ons produced as a function of thickness, and the empirical curve shows this true variation distorted by inefficiency and background.

A direct comparison of the present work with that done previously is not justifiable because of the following three reasons.

Firstly, there is no assurance that the conditions under which the results are obtained are identical. Such factors as different telescope geometry or imposed lower cut-off momentum of the penetrating particles as well as minimum energy required by the knock-ons to be detected, would alter the shape of the curve.

Secondly, some of the earlier results are not correlated with the number of penetrating primaries but rather the variation in the number of secondaries is given as a variation in counting rate (70, 71).

Thirdly, in some cases the study was made in lead only and the curve would not be expected to be the same for different materials (72, 73).

Nonetheless as far as the general shape of the curve is concerned, there is good agreement between the present and earlier work except for that of van Pittius

and van Heerden (73). However, it is very difficult to attribute the functional form of thickness dependence as determined by these authors as representing knock-on production. Their curve, showing the number of secondaries per 1000 penetrating particles as a function of the thickness, rises quickly from a background value and reaches a maximum at a thickness of about 3 cm. of lead. The curve then falls off slowly to a minimum value at a thickness of about 12 cm. The experimenters attribute this maximum to be due to accompanying soft radiation. For thicknesses greater than 12 cm. their curve shows a gradual increase in the number of secondaries with an increase in thickness of material until saturation is reached at approximately 22 cm. of lead. This second increase is interpreted as showing the variation in knock-on production and is extrapolated to zero thickness to obtain the overall dependence on thickness.

If this second increase of 18 secondaries per 1000 mesons is in fact due to knock-ons then they must have been produced in the thickness between 12 and 22 cm. of lead. This conclusion is arrived at because there seems to be no plausable explanation by which the additional lead could influence the production of knock-ons in the lower 12 cm. Assuming the secondaries are electrons they must have energies sufficient to penetrate 12 cm. of lead in order to be detected. This requires that their secondaries be

produced with energies of the order $2 \cdot 10^4$ mc^2 (90). Knock-on electrons with energies greater than this value can be produced only by mesons with momenta in excess of 100 Mc. The average number of mesons with momenta greater than this value contained in a sample of 1000 mesons taken at sea level is 73 according to the differential momentum spectrum as given in section 3.6. Thus , in order to attribute this second increase to the production of knock-on electrons requires a probability of production of the order of $2 \cdot 10^{-3}$ per gm.-cm.$^{-2}$.

This value can be compared with the expected value obtained from equation [8] of section 3.6 which gives the theoretical probability of a meson of momentum p producing a knock-on electron with energy in excess of E_o. A maximum value of this probability for the conditions applicable for comparison can be obtained by substituting the appropriate value of C for lead, and the value $2 \cdot 10^4$ mc^2 for E_o, then letting the momentum p tend to infinity. This gives a probability of production of 10^{-5} per gm.-cm.$^{-2}$. This calculated probability is two orders of magnitude too small to account for the observed increase.

Since there is no apparent reason to doubt the validity of the theory of relativistic collisions or of the rate of energy loss by electrons, one is forced to one of the two following conclusions. Either the theoretical

expression for the probability of knock-on production is incorrect for very close collisions or the secondaries observed by van Pittius and van Heereden are not knock-on electrons.

It seems unreasonable to credit the discrepancy in the two values of the production probability to the first mentioned possibility in the light of the results obtained by W. D. Walker (66). This worker investigated the integral energy spectrum of electrons knocked on by mesons and found that the theoretical cross-section fits the experimental data for knock-on energies of a few Mev. up to energies of the order of a Bev. In particular he found that during 10000 traversals of mesons with momenta greater than 1.5 Bev./c only two knock-on electrons with energies greater than 1 Bev. emerged from a one-inch plate of carbon. Furthermore by extrapolating his integral spectrum of knock-ons to an energy of 10 Bev. ($2 \cdot 10^4$ mc^2) and using the approximate number of mesons in his sample that could transfer energy in excess of this amount to the knock-on, one obtains a value of $2 \cdot 10^{-5}$ per gm.-cm.$^{-2}$ for the probability of production of a knock-on with energy greater than $2 \cdot 10^4$ mc^2 by a meson. This value is in excellent agreement with the calculated value above. One is therefore left with the conclusion that the secondaries observed by van Pittius and van Heereden are not knock-on electrons. This, then would account for the vast

discrepancy between the production curve observed by these authors and the other workers.

Although it is impossible to compare directly the present experimental results with those for aluminum obtained by Tongiorgi (70) and by Clay and Venema (71) an indirect comparison can be made by means of the calculated curve. The calculated curve does not represent the exact conditions under which the two earlier experiments were carried out. Nonetheless the differences would not be expected to be of such a magnitude as to alter the shape of the curve drastically. It, therefore, seems reasonable to compare the experimental results of these two workers for the production in aluminum with the present calculated curve. The most conclusive way of doing this is to plot the experimental values obtained for the various thicknesses against the calculated value for the same thickness as shown in Figure 12. The curves so obtained are essentially linear as would be expected if there was a true correlation between the calculated and experimental values. The two curves attributed to the work of Tongiorgi are obtained from the results of the two telescope configurations employed during his observations. The linearity of these curves is not as certain as that for the results of Clay and Venema because there are only three points to define the curve in each case.

Finally, since both the present and earlier

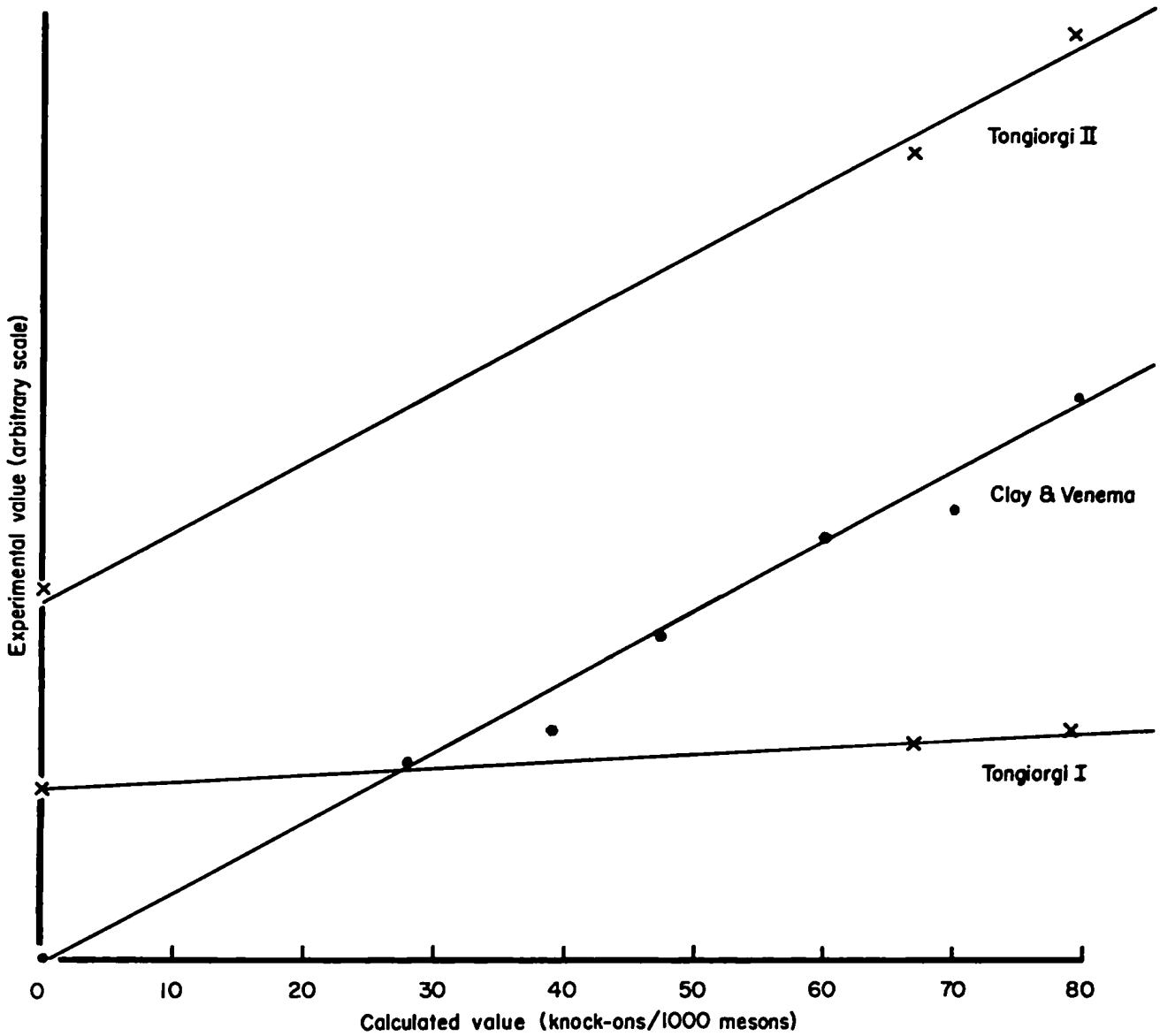

FIG. 12. Comparison of present calculated knock-on frequency with earlier experimental results

experimental production curves agree with the calculated curve with regard to the form of the variation, it can be concluded that the experimental results must be in mutual agreement. However with regard to the absolute number of knock-ons produced at any thickness no definite conclusion can be made.

The empirically determined percentages of sea level mesons with momenta greater than 4 Mc, which are accompanied by knock-on electrons with energies greater than 1.3 mc^2, upon emerging from a thickness of various materials, corrected for zero thickness background and geometrical detection efficiency, are given in Table XII.

TABLE XII

Fraction of mesons emerging from a thickness of material that are accompanied by knock-on secondaries.

Material	Thickness in gm.-cm.$^{-2}$	% Mesons accompanied by knock-ons
C	11.2	7.6 ± 0.8
Al.	12.8	8.2 ± 0.7
Fe.	10.5	6.7 ± 0.7
Pb.	10.1	4.8 ± 0.6

The results quoted above are in agreement as to the order of magnitude with the measurements of other workers. This is all that can be expected considering the possible differences that could exist in experimental arrangements.

CHAPTER 4

GENERAL DISCUSSION

4.1 The Absorption Experiment

The absorption experiment seems to the author to be quite straight forward. The only dissatisfaction with the results obtained is that no definite reason can be given to account for the very pronounced anomalous maximum observed in the earlier work. Nonetheless because of the strict requirements imposed on the operation of the equipment and the excellent stability of the telescope during the second experiment as opposed to the earlier, the author is confident that curve II of Figure 1 (page 113) is the more realistic representation of the absorption. This conclusion is made even more inevitable when the results of Heyland and Duncanson (59) and Kennedy (60) are considered. The present results should be somewhat better than those of the above mentioned authors because of the anticoincidence counters employed to reduce scattering and side shower effects.

Because of the reliability of the later results on the absorption one is forced to conclude that the anomaly is not real and to be content with the suggestion that it may have been caused by insufficient attention to the proper arrangement of absorbers or by changes in atmospheric conditions.

4.2 The Knock-on Experiment

It is an obvious fact that this investigation could have been done much more quickly and accurately with artifically produced mesons, because of the greater intensity and better control of experimental conditions. This is a general criticism that could be made of almost all experiments that use cosmic radiation simply as a source of mesons in which high energy events are not of importance.

Besides this defect, the major direct criticism of the method of studying the knock-on production reported herein is the fact that the simple apparatus employed does not permit positive identification of the primary and secondary particles as could be done with more elaborate equipment. However, the author feels that the arguments presented in section 3.5 are sufficient to establish to a high probability that the phenomenon studied is in fact the production of knock-on electrons by mu-mesons. This conclusion is made even more convincing by the good agreement between the experimental observations and that expected for knock-on electron production as calculated theoretically.

It is unfortunate that the statistics are not better so as to make the agreement more conclusive. The possibility of improving the statistics, either by increasing the aperture of the telescope or by extending

the time of observation, has been considered. However, the first way defeats the purpose of the experiment because an increase in aperture produces a decrease in definition (the beam would not be as well collimated). This would increase the difficulty of interpretation of events and make theoretical calculations almost impossibly complicated. The second method of decreasing the statistical errors is not practical since to reduce the standard deviation by a half requires the time of observation to be increased by a factor of four. The gain in accuracy does not warrant the additional expense and trouble that is involved in an extension of the observation time.

The results of this investigation allow the conclusion that the experimental and theoretical probabilities for the production of knock-on electrons by mu-mesons in aluminum are in mutual agreement to within 5%.

Furthermore a valid method has been indicated for calculating the percentage of mesons that, upon emerging from a thickness of aluminum, would be accompanied by knock-on electrons. This has been shown to hold only up to a thickness of 12.8 gm.-cm.$^{-2}$ of aluminum. However, it is reasonable to assume that with the proper electron range function these calculations could be extended to other thicknesses and other materials. This, thereby, provides a ready method of estimating the effect of knock-on

production in other types of experiments where such events could produce false coincidences.

APPENDIX

On Anomalies in the Absorption of Cosmic Rays in Lead

Irregularities in the absorption curve of cosmic rays in lead have been reported by several authors (1, 2, 3, 4, 7, 8, 10, 11), using counter telescopes. More recently, other workers (5, 6, 9), who were looking specifically for these anomalies, failed to find them. Our initial experiment (7), using a single triple coincidence telescope and point-by-point scanning of the absorption curve, yielded an anomalous maximum as shown in curve I (Fig. 1). Since it was felt that day-by-day fluctuations might have been responsible for this maximum, we have repeated our experiment, determining four points on the absorption curve simultaneously. Curve II, so obtained, shows no evidence for any anomalies and supports the careful measurements of Heyland and Duncanson (6).

The telescope configurations used in the present experiment are shown in the inset of Fig. 1. The counters were of the external cathode type, with plateaus of about 250 volts and an average slope of 0.02% per volt. Arrangement (*a*) defines four triple coincidence telescopes with the side counters in anticoincidence. The rates 123–7, 124–7, 125–7, and 126–7 were recorded. The anticoincidence counters were used to reduce the differences in the telescope apertures and the

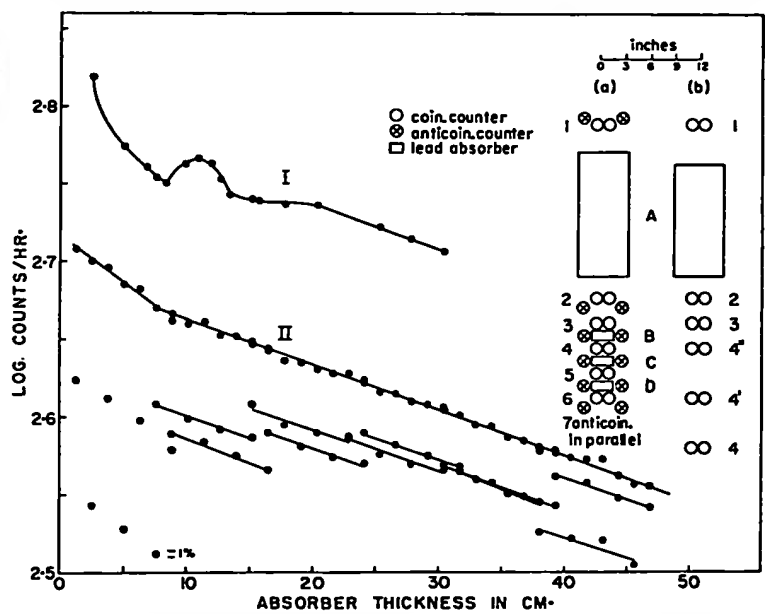

FIG. 1. Absorption curve of cosmic rays in lead, showing telescope arrangement inset.

errors due to scattering and side showers. The results for four absorber thicknesses were obtained simultaneously by placing 1 in. thickness of lead at *B*, *C*, and *D*. Absorber *A* was varied to give both overlapping and adjacent four-point segments of the absorption curve. The rates of the different telescopes were normalized to that of 123–7 by multiplying by the appropriate "geometry factors". These factors, which are the ratios of the counting rates of the telescopes with no absorbers in positions *B*, *C*, or *D*, were constant in time and independent of lead thickness in position *A*. Since the factors were also directly proportional to the ratios of the angular apertures, it was concluded that the efficiencies of the telescopes were equal and the factors were truly geometric.

The final results of the absorption measurements are also presented in Fig. 1. The four-point segments, corrected for geometry only, are shown in the lower part of the graph. Each point is based on approximately 15,000 counts. The internal consistency of the points defining a segment is much better than that expected from statistical considerations because the counting rates are not completely independent. However, the variations in the segments are, in some cases, much greater than would be expected from random counting. These large differences are interpreted as being caused by atmospheric fluctuations, a source of error that was not taken into account in our earlier work. The end points of the segments were fitted together to give curve II of Fig. 1. No corrections for accidental and shower rates were made since these were at all times less than 1% of the observed rate.

Since in our earlier work the absorber was above the telescope (as for 234 of arrangement (*b*) in Fig. 1) while in the present work it was within the telescope (as for 123 of the same arrangement) it was felt that perhaps the anomalies observed were dependent on the position of the absorber relative to the telescope. However, it was found that the ratio of the rate 123 to the rate 234 taken simultaneously was independent of absorber thickness, provided the cross-sectional area of the absorber was sufficient to fill the apertures of both telescopes. The ratio became strongly dependent on absorber thickness unless this requirement was strictly adhered to.

It is concluded that within 1% there is no anomaly in the cosmic ray absorption curve for lead thicknesses up to 45 cm. Moreover, these experiments suggest that the previously observed anomalies could easily have been created by insufficient attention to the proper arrangement of absorbers or to changes in atmospheric conditions.

One of the authors (G. L. Keech) takes this opportunity to express his appreciation to the Shell Oil Company for a fellowship during the year 1952–53 and to the National Research Council for Studentships in the two succeeding years.

1. Abd El-Wahab Khalil, M. Nuovo cimento, 9: 1248. 1952.
2. Aiya, S. V. C. Nature, 153: 375. 1950.
3. Fenyves, E. and Haiman, O. Nature, 165: 244. 1950.
4. George, E. P. and Appapillai, V. Nature, 155: 720. 1945.
5. Heyland, G. R. and Duncanson, W. E. Nature, 167: 895. 1951.
6. Heyland, G. R. and Duncanson, W. E. Proc. Phys. Soc. (London), A, 66: 33. 1953.
7. Keech, G. L. M.Sc. Thesis, McMaster University, Hamilton, Ont. Oct. 1952.
8. Kellermann, E. W. and Westerman, K. Proc. Phys. Soc. (London), A, 62: 356. 1949.
9. Kennedy, W. L. Australian J. Phys. 6: 500. 1953.
10. Mazzolli de Mathov, E. Nature, 167: 192. 1951.
11. Swann, W. F. G. and Morris, P. F. Phys. Rev. 72: 1262. 1947.

Received January 17, 1955.
Department of Physics,
Hamilton College,
McMaster University,
Hamilton, Ontario.

G. L. Keech*
F. Gulbis

*Holder of a National Research Council Studentship 1954–55.

REFERENCES

1. Wilson, C. T. R. Proc. Roy. Soc. A, 68: 151. 1901.
Proc. Roy. Soc. A, 69: 277. 1901.

2. Hess, V. F. Physikal. Zeits. 12: 998. 1911.
Physikal. Zeits. 13: 1084. 1912.

3. Kolhorster, W. Deutsch Phys. Gesell. 16: 719. 1914.

4. Millikan, R. A. and Cameron, G. H. Phys. Rev. 31: 921. 1928.

5. Geiger, H. and Müller, W. Phys. Zeits, 29: 839. 1929.
Phys. Zeits, 30: 489. 1929.

6. Wilson, C. T. R. Proc. Roy. Soc. A, 85: 285. 1911.
Proc. Roy. Soc. A, 87: 277. 1912.

7. Blackett, P. M. S. and Occhialini, G. P. S. Nature, 130: 363. 1932.

8. Bothe, W. and Kolhorster, W. Naturwiss. 16: 1044. 1928.
Zeits. f. Physik, 56: 751. 1929.

9. Skobelzyn, D. Zeits. f. Physik, 43: 354. 1927.

10. Skobelzyn, D. Zeits. f. Physik, 54: 686. 1929.

11. Anderson, C. D. Science, 76: 238. 1932.
Phys. Rev. 43: 491. 1933.
Phys. Rev. 44: 406. 1933.

12. Rossi, B. Physikal. Zeits. 33: 405. 1932.

13. Bhabha, H. J. and Heitler, W. Proc. Roy. Soc. A, 159: 432. 1937.

14. Street, J. C., Woodward, R. H. and Stevenson, E. C. Phys. Rev. 47: 891. 1935.

15. Neddermeyer, S. H. and Anderson, C. D. Revs. Mod. Phys. 11: 191. 1939.

16. Yukawa, H. Proc. Phys.-Math. Soc. Japan, 17: 48. 1935.

17. Ehmert, A. Zeits. f. Physik, 106: 751. 1937.

18. Williams, E. J. and Roberts, G. E. Nature, 145: 102. 1940.

19. Rasetti, F. Phys. Rev. 60: 198. 1941.

20. Conversi, M., Pancini, E. and Piccioni, O. Phys. Rev. 71: 209. 1947.

21. Lattes, C. M. G., Occhialini, G. P. S. and Powell, C. F. Nature, 159: 694, 1947. Nature, 160: 453, 486. 1947.

22. Shapiro, M. M. Rev. Mod. Phys. 13: 58. 1941.

23. Camerini, U., Muirhead, H., Powell, C. F. and Ritson, D. Nature, 162: 433. 1948.

24. Compton, A. H. Phys. Rev. 43: 387. 1933.

25. Johnson, T. H. Rev. Mod. Phys. 10: 193. 1938.

26. Schein, M., Jesse, W. P. and Wollan, E. O. Phys. Rev. 59: 615. 1941.

27. Freir, P., Lofgren, E. J., Ney, E. P., Oppenheimer, F., Bradt, H. L. and Peters, B. Phys. Rev. 74: 213. 1948.

28. Wilson, J. G. (editor) Progress in Cosmic Ray Physics. Vol. I, page 210. New York, Interscience Publishers Inc. 1952.

29. Duperier, A. Terr. Magn. Atm. El. 49: 1. 1944.

30. Freon, A. Compt. Rend. 218: 277. 1944.

31. Fowler, P. H. Phil. Mag. 41: 169. 1950.

32. Hazen, W. E. Phys. Rev. 64: 257. 1943. Phys. Rev. 65: 67. 1944.

33. Piccioni, O. Phys. Rev. 77: 1. 1950.

34. Deutschman, M. Naturwiss. 42: 499. 1955.

35. Barkas, J. d., Smith, F. M. and Gardner, E. Phys. Rev. 82: 102. 1951.

36. Jakobson, M. J., Schulz, A. and Steinberger, J. Phys. Rev. 81: 894. 1951.

37. Marshak, R. E. Meson Physics. Page 137. New York, McGraw-Hill Book Co., Inc. 1952.

38. Panofsky, W. K., Aamodt, R. L. and York, H. F.
Phys. Rev. 78: 825. 1950.
Panofsky, W. K., Aamodt, R. L., Hadley, J. and Phillips, R.
Phys. Rev. 80: 94. 1950.

39. Kaplon, M. F., Peters, B. and Ritson, D. Phys. Rev. 85: 900. 1952.

40. Daniel, R. R., Davies, J. H., Mulvey, J. H. and Perkins, D. H. Phil. Mag. 43: 753. 1952.

41. Clark, D. L., Roberts, A. and Wilson, R. Phys. Rev. 83: 649. 1951.

42. Durbin, R., Loar, H. and Steinberger, J. Phys. Rev. 83: 646. 1951.

43. Marshak, R. E. Meson Physics. Page 145. New York, McGraw-Hill Book Co. Inc. 1952.

44. Tinlot, J. Phys. Rev. 73: 1476. 1948.
Phys. Rev. 74: 1197. 1948.

45. Brode, R. B. Rev. Mod. Phys. 21: 38. 1949.

46. Alvarez, L. W., Longacre, A., Oppen, V. G. and Thomas, R. G. Phys. Rev. 77: 752. 1950.

47. Marshak, R. E. Meson Physics. Page 204. New York, McGraw-Hill Book Co. Inc. 1952.

48. Marshak, R. E. Meson Physics. Page 219. New York, McGraw-Hill Book Co. Inc. 1952.

49. Auger, P., Maze, R. and Grivet-Meyer, T. Compt. Rend. 206: 1721. 1938.

50. Abd El-Wahab Khalil, M. Nuovo Cimento, 9: 1248. 1952.

51. Aiya, S. V. C. Nature, 153: 375. 1950.

52. Fenyves, E. and Haiman, O. Nature, 165: 244. 1950.

53. George, E. P. and Appapillai, V. Nature, 155: 726. 1945.

54. Kellermann, E. W. and Westerman, K. Proc. Phys. Soc. (Lond.), A, 66: 33. 1953.

55. Mazzolli de Mathov, E. Nature, 167: 192. 1951.

56. Swann, W. F. G. and Morris, P. F. Phys. Rev. 72: 1262. 1947.

57. Heyland, G. R. and Duncanson, W. E. Nature, 167: 895. 1951.

58. Keech, G. L. M. Sc. Thesis, McMaster University, Hamilton, Ontario. October, 1952.

59. Heyland, G. R. and Duncanson, W. E. Proc. Phys. Soc. (Lond.), A, 66: 33. 1953.

60. Konnedy, W. L. Aust. J. Physics, 6: 500. 1953.

61. Hazen, W. E. Phys. Rev. 64: 7. 1943.

62. Seren, L. Phys. Rev. 62: 204. 1942.

63. Swann, W. F. G. and Ramsey, W. E. Phys. Rev. 57: 749. 1940.

64. Nassar, S. M. and Hazen, W. E. Phys. Rev. 69: 298. 1946.

65. Clay, J. Physica, 13: 433. 1947.

66. Walker, W. D. Phys. Rev. 90: 234. 1953.

67. Brown, W. W., McKay, A. S. and Palmatier, E. D. Phys. Rev. 76: 506. 1949.

68. Lovati, A., Mura, A. and Succi, C. Nuovo Cimento, 11: 92. 1954.

69. Calylioti, C., Sciuti, S. and Giglli, A. Nuovo Cimento, 12: 851. 1955.

70. Tongiorgi, V. Nuovo Cimento, 3: 342. 1946.

71. Clay, J. and Venema, H. Physica, 10: 735. 1943.

72. Bassi, P. and Lori, A. Nature, 163: 410. 1949.

73. van Pittius, E. van A. and van Heerde n, I. J. Physica, 19: 1. 1953.

74. Katz, L. and Penfold, A. S. Rev. Mod. Phys. 24: 28. 1952.

75. MacKnight, M. L. and Chasson, R. L. Rev. Sci. Inst. 22: 700. 1951.

75A. Maze, R. J. Phys. Radium, 7: 164. 1946.

76. Jenkins, R. O. and Taylor, R. W. Rev. Sci. Inst. 24: 73. 1953.

77. Wilson, Jr., E. B. An Introduction to Scientific Research. Page 191. New York, McGraw-Hill Book Co. Inc. 1952.

78. Wilson, Jr., E. B. An Introduction to Scientific Research. Page 252. New York, McGraw-Hill Book Co. Inc. 1952.

79. Eckart, C. and Shonka, F. R. Phys. Rev. 53: 752. 1938.

80. Ballam, J. and Lichtenstein, P. G. Phys. Rev. 93: 851. 1954.

81. Mylroi, M. G. and Wilson, J. G. Proc. Phys. Soc. (Lond.), A, 64: 404. 1951.

82. Whittemore, W. L. and Shutt, R. P. Phys. Rev. 86: 940. 1952.

83. Marshak, R. E. Meson Physics. Chapter 7. New York, McGraw-Hill Book Co. Inc. 1952.

84. Hayakawa, S. and Tomonaga, S. Prog. Theor. Phys. 4: 496. 1949.

85. Hereford, F. L. Phys. Rev. 75: 923. 1949.

86. Bhabha, H. J. Proc. Roy. Soc. (Lond.), A, 164: 257. 1938.

87. Massey, H. J. and Corben, H. C. Proc. Camb. Phil. Soc. 35: 463. 1939.

88. Rossi, B. Rev. Mod. Phys. 20: 537. 1948.

89. Caro, D. E., Parry, J. K. and Rathgeber, W. D. Nature, 165: 689. 1950.

90. Greisen, K. Phys. Rev. 75: 1071. 1949.